ELSEVIER

RESEARCH: Review

Thermally drawn advanced functional fibers: New frontier of flexible electronics

Wei Yan [1], Chaoqun Dong [2,†], Yuanzhuo Xiang [3,†], Shan Jiang [4], Andreas Leber [2], Gabriel Loke [5], Wenxin Xu [3], Chong Hou [3], Shifeng Zhou [6], Min Chen [7], Run Hu [8], Perry Ping Shum [9], Lei Wei [9], Xiaoting Jia [4], Fabien Sorin [2], Xiaoming Tao [10], Guangming Tao [3,*]

[1] Research Laboratory of Electronics, Massachusetts Institute of Technology (MIT), Cambridge, MA 02139, USA
[2] Laboratory of Photonic Materials and Fibre Devices (FIMAP), Institute of Materials, Ecole Polytechnique Fédérale de Lausanne (EPFL), Lausanne 1015, Switzerland
[3] Wuhan National Laboratory for Optoelectronics and School of Optical and Electronic Information, Huazhong University of Science and Technology, Wuhan 430074, China
[4] Bradley Department of Electrical and Computer Engineering, Virginia Polytechnic Institute and State University, Blacksburg, VA 24060, United States
[5] Department of Materials Science and Engineering, Massachusetts Institute of Technology (MIT), Cambridge, MA 02139, USA
[6] State Key Laboratory of Luminescent Materials and Devices, School of Materials Science and Engineering, South China University of Technology, Guangzhou 510640, China
[7] Wuhan National Laboratory for Optoelectronics and School of Computer Science and Technology, Huazhong University of Science and Technology, Wuhan 430074, China
[8] State Key Laboratory of Coal Combustion, School of Energy and Power Engineering, Huazhong University of Science and Technology, Wuhan 430074, China
[9] School of Electrical and Electronic Engineering, Nanyang Technological University, 50 Nanyang Avenue, 639798 Singapore, Singapore
[10] Institute of Textiles and Clothing, The Hong Kong Polytechnic University, Hong Kong 999077, China

Electronic devices are evolving from rigid devices into flexible and stretchable structures, enabling a seamless integration of electronics into our everyday lives. The integration of a variety of electronic materials within thermal-drawn fibers has emerged as a versatile platform for the fabrication of advanced functional fiber electronics. This approach exploits the thermal drawing of a macroscopic preform, where functional materials or prefabricated devices are arranged at a prescribed position, yielding kilometers of electronic fibers with a sophisticated architecture and complex functionalities in a very simple and scalable manner. A single strand of fiber that incorporates materials with disparate electronic, optoelectronics, thermomechanical, rheological and acoustic properties can see objects, hear sound, sense stimuli, communicate, store and convert energy, modulate temperature, monitor health and dissect brains. Integrating these electronic fibers into fabrics, ancient yet largely underdeveloped forms, is setting a stage for fabrics to be the next frontier in computation and Artificial Intelligence. Here, we critically review the development of thermally drawn fiber electronics and highlight their unique opportunities in communications, sensing, energy, artificial muscles, 3-D printing, healthcare, neuroscience as well as in-fiber materials fundamental research. We conclude

* Corresponding author.
E-mail address: Tao, G. (tao@hust.edu.cn)
† These authors contribute equally to the work

https://doi.org/10.1016/j.mattod.2019.11.006

some perspectives for realizing an analogue of "Moore's law" in fibers and fabrics and the remaining challenges for future research.

Introduction

Electronic devices used to be rigid, planar and cumbersome. Decades of research have led to the emergence of miniaturized, soft, flexible and stretchable electronics. Fundamental breakthroughs in materials, mechanics, device morphologies and geometries, as well as the device properties, endow these electronics with unique applications. Examples include medical devices implanted in the human body for therapeutic treatment, neural probes that integrate multiple functionalities to dissect neural circuits in the brains, biocompatible, skin-interfaced sensors for physiological analysis, artificial intelligence for soft robotics, energy harvesting using nanogenerators, e-textiles that integrate wearable batteries and supercapacitors. Among these electronic devices, fiber-shaped electronics hold special promise for a variety of unique applications due to their peculiar geometry, aspect ratio mechanical properties or wearable and washable attributes [1–16]. However, the fabrication of fiber-based electronic devices, especially with integrated multimaterials and intricate architectures, is quite challenging initially. This is in part because the well-established processing techniques, such as photolithography and nanoimprinting, typically used for fabricating 2D devices, are not applicable for the fibers with highly-curved geometries. Therefore, several fiber processing strategies, such as numerous coating techniques [17], physical and chemical vapor deposition [18], electrospinning [19], physical convolution and wrapping [20], printing [21], and various patterning techniques [22] have been developed. Different from the planar electronic devices with typical stacking structures, these fiber devices are featured with unique coaxial [23–24], twisted [25–26], and interlaced [27] configurations. Great effort on fiber studies has led to a variety of fiber architectures and functionalities, such as biosensors [28], supercapacitors [29–30], batteries [31–32], piezo/triboelectric generators [33], solar cells [34], light-emitting electrochemical cells [35], light-emitting devices [36]. Despite the capability of exploiting various well-established materials, most of the techniques are very complex and involve multiple steps. Thus, the resulting fiber electronics have simple, limited functionalities. The performance might decay or vary along the fiber length. Moreover, it remains technologically challenging for these techniques to scale to a large area. A few decades ago, a new family of functional fibers that integrated different materials with disparate optical, electronic, and optoelectronic properties emerged [1]. The method at the heart of the fabrication exploits thermal drawing, a typical approach for producing optical fibers in industry. Designing the architectures in a macroscopic scaled-up model of the fiber called preform where desirable electronic materials are well-positioned, thousands of kilometers of electronic fibers that maintain the preform cross-section with sophisticated structures and complex functionalities beyond telecommunication are produced in a very simple and unprecedentedly scalable way [37]. As the preform is structured at the millimeter scale, multiple mutually-independent devices can be arranged in place and the subsequent preform-to-fiber drawing results in a single fiber with a high density of devices and various functionalities. Control over the scalability allows for electronic fibers with exceptionally tunable feature size spanning several orders of magnitude: from micrometers to a few nanometers. Besides maintaining the axial symmetry during draw, fiber itself can act as a unique platform via breaking symmetry for the synthesis of novel technologically important materials, the formation of unusual micro-/nanoscale geometries and architectures, the construction of unique devices as well as fundamental investigation of many interesting topics in materials science, micro-/nanotechnology and condensed physics. Such features are unachievable with other existing fiber-processing methods. In this review article, we examine the advances of thermally drawn fiber electronics that may allow electronics to be seamlessly integrated into our everyday lives in the future, as schematically shown in Fig. 1. We first introduce the principle and processing method of thermal drawing. We then present the applications of fiber electronics in optics, communications, sensing, imaging, energy harvesting and storage, artificial muscles, bioengineering and neuroscience, micro- and nanofabrication as well as novel materials and structure formation. Finally, we discuss the perspective and challenges that exist in developing practical applications and exploring fundamental research. In particular, we provide our insights into how future fabrics will be reshaped by thermally drawn electronic fibers, and how fabrics will be the next frontier in computation and Artificial Intelligence.

Principles of thermal drawing

Hundred-of-kilometer-long optical fibers are typically produced by thermoplastically pulling a preform at the softening temperature of silica. With the same simple technique, a new family of thermally drawn fibers can be fabricated. The preform can be fabricated via many approaches, such as the thin-film rolling technique for cylindrical fibers, extrusion, the stack-and-draw approach, assembling different components together via consolidation in a hot press and additive manufacturing [41]. The preform is then fed into a furnace where materials soften or melt. An external force applied by a capstan pulls the soft preform into fibers, and the size of the fibers which can be controlled by the drawing temperature of the hottest zone of the furnace, the feeding speed of the preform, and the drawing tension. In Table 1 we highlight the representative work showing the history development of the thermally drawn fibers. The earlier thermally drawn fibers exhibit translational symmetry where both fiber materials and geometries are identical to those in the fiber preform [42–43]. Several constraints are set to thermally co-draw different materials with disparate thermo-mechanical, physical and rheological properties, as detailed in recent review articles [37,41]. Some recent research has focused on breaking the translational

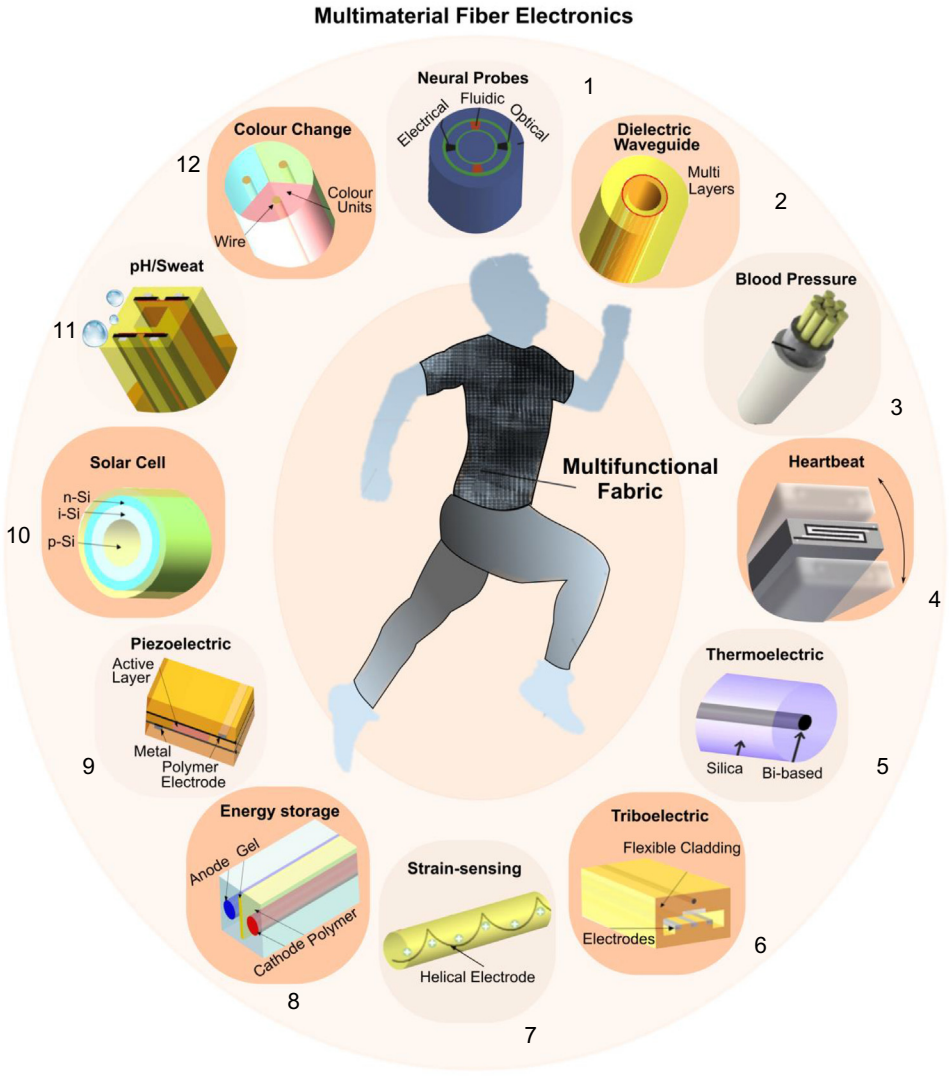

FIGURE 1

A schematic of multifunctional smart fabric integrated from multimaterial fiber electronics: (1) Fiber neural probe transmits lights, records bioelectrical signals, and delivers chemicals. Reproduced with permission [38].Copyright 2015, Nature Publishing Group. (2) All dielectric photonic bandgap fiber acting as surgical tool for transmitting high-power laser light. (3) Fiber blood pressure sensor detects the systolic blood pressure and the diastolic blood pressure. Reproduced with permission [39]. Copyright 2015, Wiley-VCH. (4) Piezoelectric fiber monitors heart beating rate. (5) Thermoelectric fiber maps the shell temperature. (6) Triboelectric fiber harvests mechanical energy from body movements. (7) Deformation sensing fiber detects strain change. (8) Fiber supercapacitor stores energy harvested from piezoelectric fiber and triboelectric fiber. (9) Piezoelectric fiber performs pulse and tactile sensing. (10) Photovoltaic fiber transfers solar energy to electrical energy. (11) Optoelectronic fiber analyzes the sweats during sports. Reproduced with permission [40]. Copyright 2012, Wiley-VCH. (12) Color-changing fiber spontaneously changes color upon external stimulation under different environment.

symmetry. The methods include the introduction of chemical reactions [44] or a phase transformation during thermal drawing [1,45], the incorporation of functional materials that cannot be co-drawn with other fiber materials into the channels, holes or pockets in the as-drawn fibers [40], post-processing of as-drawn fibers via different physical or chemical treatments such as heating [46–47], laser irradiation [48–49], solvent soaking [50] and cold drawing [51], and direct in situ incorporation of well-established functional materials and high-performance devices into fibers during thermal drawing [52]. All of these developments have led to the emergence of new thermally drawn fibers with increasingly sophisticated architecture and complex functionalities.

Photonic bandgap fibers

In the early stage, tremendous efforts were focused on developing photonic fibers capable of transmitting light in a way unachievable with traditional silica optical fibers or photonic crystal fibers. To better highlight the emergence of electronic fibers, in this section, we first introduce the concept of photonic bandgap (PBG) fibers and their applications in the delivery of mid-infrared (MIR) light [77]. Integrating PBG structure with electronic and optoelectronic functionalities within a single fiber delivers unprecedented applications in optics, sensing and healthcare, as we elaborated in the Section "Electronic fibers".

TABLE 1

Representative work showing the development of thermally-drawn multimaterial fiber electronics.

Fibers	Key materials	Applications	References
Photonic bandgap fibers	Dielectric polymer PES, chalcogenide glass As_2Se_3	Omnidirectional reflection and light guidance	[42–43]
Optoelectronic fibers	As-Se-Te-Sn, Sn	Photosensing	[53]
	Chalcogenide semiconductor GAST, Sn	Self-monitoring high-power optical transmission	[54]
	Chalcogenide semiconductor As-Se-Te-Sn, metal Sn-Ag	Detection of light direction, measurement of the amplitude and phase of an electromagnetic field	[55]
	As-Se, As-Se-Te	Detection of light angle, wavelength and lensless imaging	[56]
	As-S, PC	Azimuthally polarized radial fiber laser	[57]
	Single crystal Se nanowires	High-performance photosensing, fluorescence imaging	[50]
	LED, p-i-n diodes	Optical communications	[52]
Electronic fibers	GAST, Sn	Thermal sensing	[58]
	Piezoelectric polymer, nanocomposite CPC, Indium	Ultrasound detection	[59]
	As-Se-Te, Sn	Field-effect transistor	[46]
	Ga-Ge-Te	Memory switching	[60]
	Se-S, SnPb	Chemical sensing	[40]
	SEBS, liquid metal, nanocomposite cPE	Deformation sensing	[61]
	P(VDF–TrFE–CFE), cPE	Electromechanical actuation	[62]
	Cu wires, cPE	Microfluidics for high-throughput cell separation	[63]
	Cu-As-Te-Se	Thermoelectric sensing and cooling	[64]
	elastic COCe, high-density PE	Artificial muscle	[65]
Multifunctional fibers	Optics, electronics, chemicals	Neural interfacing	[38,66]
In-fiber micro- and nanofabrication	Metals. semiconductor, polymers	Micro- and nanowires, structured spheres, semiconducting sphere-based optoelectronics	[67–71]
Fiber synthesis	Se-S, Sn-Zn, ZnSe	New devices formation	[44–45,72–73]
	Al, SiO_2, Si	New materials formation	
	PVdF, PCL	Porosity formation	
Laser structuring	Si, Ge, SiGe,	Single crystal formation, compositional tailoring, bandgap modification,	[48,74–75]
Device ink	Functional fibers	3-D printed devices	[76]

The two typical atmospheric transmission windows contains a large quantity of molecular fingerprints in the MIR range, as shown in Fig. 2a. The MIR waveband is of great significance in medical [78], industrial [79], and military [80] applications. The rapid developments of typical MIR detectors and MIR sources [81] are outlined in Fig. 2a. Little attention has been devoted to the transmission medium. Typical MIR media are the light-guide arm [82], metal-doped hollow-core tube [83] and gas cell illustrated in Fig. 2b. However, the lack of flexibility of these transmission media greatly limits their applications.

To meet the requirements for flexibility and low loss in sensing and materials processing, hollow-core micro-structured optical fibers (HC-MOFs) based on IR-transparent materials have been developed. Bragg fibers are the first HC-MOF proposed [42], which confine light to a hollow core by a PBG mirror comprising alternating layers. The alternating layers form a photonic bandgap, in which light with a specific frequency cannot transmit along the fibers. The main influencing factors of the photonic bandgap are the thickness and refractive index of each layer, which determine the optical properties of the Bragg fibers. In contrast to other PBG fibers, Bragg fibers are easily fabricated, and their photonic bandgaps are easily controlled.

Fig. 2c describes the fabrication process of such PBG fibers [42]. The structure and transmission spectrum of one typical fiber is shown in Fig. 2c. Indeed, the transmission window ranges from 0.75 to 10.6 μm depending on the photonic bandgap, and the transmission loss could be reduced to less than 1 dB/m by optimizing the fabrication process, which is small enough to be applied in sensing and power transmission. A series of applications have thus been developed, such as CO_2 laser transmission for surgery tools [42], optical resonators [84–85] and self-monitoring high-power transmission [54]. In particular, the capability of transmission of high-power CO_2 laser with an inappreciable loss using PBG fibers directly leads to the foundation of OmniGuide, a company developing and commercializing minimally-invasive surgical tools. To date, the PBG fiber still provides significant advantage for CO2 laser transmission over the state-of-the-art hollow-core negative-curvature photonic crystal fiber that exhibits 2.1 dB/m attenuation at 10.0 μm [86] two times higher than that the PBG fiber.

Electronic fibers

Electronic devices are constructs that manipulate the electron flow for signal processing and system control. Prominent electronics include transistors, diodes, integrated circuits and optoelectronics. In this section, we will review electronic fibers in a wide range of application in modulating azimuthal laser intensity distribution, sensing various deformation stimuli such as touching, stretching, bending and twisting, detecting acoustic

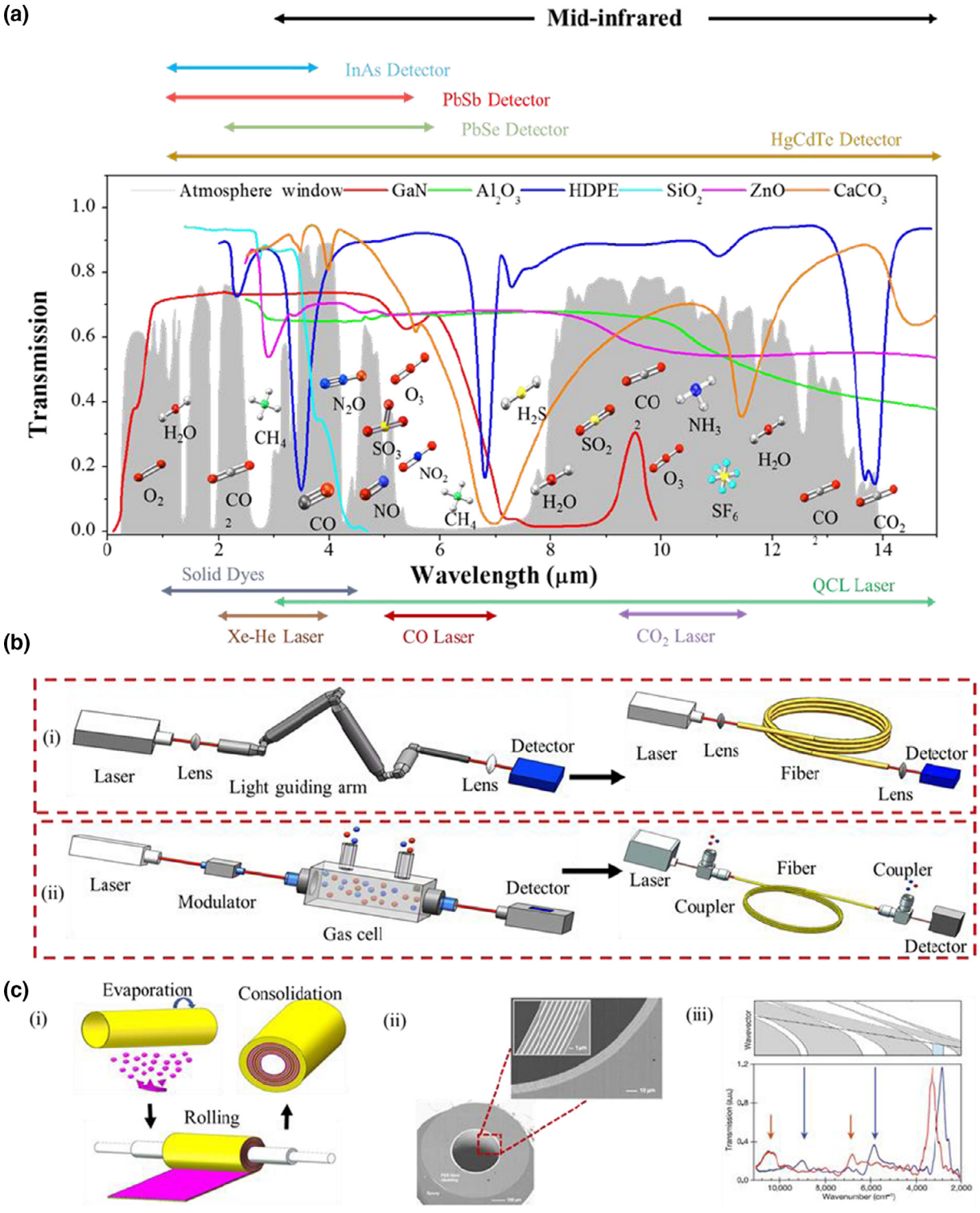

FIGURE 2

(a) The importance of IR waveband: a large quantity of molecular absorption peaks [87] and typical materials transmission spectrum such as metallic oxide (Al_2O_3) [88], semiconductor (ZnO) [89], polymer (HDPE) [90], glass (SiO_2) [91], crystal (GaN) [92], etc. The wavelength range of conventional infrared detections [93–95] and laser [96,97]. (b) The infrared light transmission and gas sensing systems with different medium. (i) Conventional infrared laser transmission system based on light guiding arm and the flexible optical fiber-based light transmission system for wearable application. (ii) The infrared gas-sensing system based on gas cell and the more flexible and compact Bragg fiber-based gas cell for wearable application. (c) The fabrication, structure and photonic bandgap of Bragg fibers. (i) Evaporating the high refractive index material (As_2Se_3, refractive index of 2.8) onto the low refractive index material (PEI, refractive index of 1.55), rolling the bilayer and consolidating it under vacuum to get Bragg fiber preform, which is later elongated into Bragg fiber. (ii) The transmission spectrum of a Bragg fiber. Reproduced with permission [42]. Copyright 2002, Nature Publishing Group. (iii) SEM image of Ta Bragg fiber. Reproduced with permission [42]. Copyright 2002, Nature Publishing Group.

signals via piezoelectric effect, creating actuation via energy conversion, forming capacitors, ovonic memory-switching effects and field-effect transistors, sensing and positioning heat, detecting radiation, and acting as strain-programmable artificial muscles.

Electronic fibers for modulating laser emission

Optofluidic fiber lasers, which integrate aqueous gain medium and micrometer-sized fiber cavities, have greatly contributed to the development of miniaturized optical devices for integrated biomedical analysis systems due to the simple manipulation of liquid solutions, minimal invasion, low pump energy consumption, great compactness, and flexibility in the design of fiber cavities. Depending on the fiber geometry and configuration, the laser can emit from the aqueous gain medium either along or perpendicular to the fiber axis. In particular, cylindrically symmetric laser emission in the transverse plane of the fiber axis is of great interest for applications of omnidirectional imaging, biomedical detection and photodynamic therapy, providing a larger laser emission surface area than the common fiber laser emission/guidance from a relatively small area along the fiber axis. To expand the applications of omnidirectional lasers, in-fiber microfluidic cylindrically symmetric radial emission is demonstrated as follows.

As shown in Fig. 3a, the hollow annular multilayered cavity consists of a 35-layer alternating structure of chalcogenide glass $As_{25}S_{75}$ and polycarbonate [57,98]. Groups of three pockets with prescribed dimensions are machined in the polycarbonate cladding. The two outer pockets are filled with conductive carbon-loaded polyethylene (CPE) strips while the center pocket is left empty. The composite structure is drawn under high stress, yielding an axially invariant, rotationally symmetric, photonic bandgap fiber cavity with a transmission bandgap centered near 550 nm. The fiber core is surrounded by four electrically addressable microfluidic channels embedded in the fiber cladding.

The fiber laser gain medium is Rhodamine 590, which is axially pumped by the second harmonic (532 nm) of an Nd:YAG laser. The laser wavefront emitted from the fiber core appears as an axially collimated ring-like beam in the far field. The cylindrical symmetry of the emission stems from the isotropic fluorescence of the dye and its coupling to the fiber cavity modes. Above the threshold, a purely azimuthally polarized beam emerges from the PBG fiber cavity, which indicates coupling to specific low-threshold fiber modes. Furthermore, a microfluidic pump is utilized to transport organic dye-doped water plugs inside the fiber core. The internal surface of the fiber core is hydrophobic and is not wet by the aqueous plug, which remains intact during a rapid movement. To use the intrinsic radial emission and azimuthal polarization state in a useful manner, an approach that facilitates directional intensity control within a complete 2π radians of control is demonstrated. By infiltrating the hollow microchannels with liquid crystals (LCs), a novel hybrid fiber device is created that can modulate the coherent laser emission with a maximum extinction ratio of ~9 dB, as shown in Fig. 3b.

However, the fast bleaching of the organic dyes limits the lasing performance under long exposure times and further deteriorates in a laser cavity because both the pumping energy and emission intensity are high in a cavity. On the other hand, semiconductor quantum dots (QDs) have enabled intensive studies as alternatives to organic dyes in light-emitting diodes, biosensing, imaging, and versatile lasers, providing the unique advantages of being less susceptible to photobleaching, great tunability over a wide spectra range, temperature insensitivity to the lasing threshold, broad excitation band and narrow emission peaks. Given the premium benefits of QDs as a gain medium and the flexibility of optofluidic fiber laser configurations, the realization of a purely radial emission QD fiber laser with a fixed azimuthal polarization direction is achieved as follows [99]. Cylindrically symmetric laser emission is obtained by axially pumping a liquid gain medium in the hollow cavity of a PBG fiber with a nanosecond Nd:YAG laser at 532 nm. The multilayer PBG consists of a hollow air core surrounded by 25 annular alternating layers of high-index chalcogenide glass $As_{25}S_{75}$ and relatively low-index PC and a pure PC cladding. First, a segment of QD-doped hexane solution infiltrates into the hollow core of the PBG fiber by capillary forces to act as the gain medium. A linearly polarized Nd:YAG laser with a pulse duration of ~5 ns is used to axially pump the gain medium. The light emission from the fiber cavity is in the transverse plane with respect to the fiber axis with cylindrical symmetry, as shown in Fig. 3c. The narrow emission peaks in the spectra confirm the lasing phenomenon and indicate that the isotropic spontaneous emission is coupled to specific low-threshold laser modes supported by the cylindrical fiber resonator. The lasing threshold is estimated to be ~238 μJ/pulse by comparing the relationship between the peak intensities and pump pulse energies, as plotted in Fig. 3d. The spacing between the adjacent lasing peaks is measured to be approximately 0.58 nm for the fiber core with a diameter of ~250 μm, as shown in Fig. 3e. Furthermore, the FWHM of the individual lasing peak is approximately 0.16 nm, indicating a high Q factor of ~4000. This Q factor value is one order of magnitude higher than that of the dye-doped counterpart, indicating a more promising lasing performance employing QDs as the gain medium. It should be noted that the study of novel laser materials is attracting lots of interest and promising for the development of next-generation all-fiber photonic systems [100–107].

Stretchable and soft fibers for deformation sensing

Coupling mechanics and electronics in single devices is an effective strategy to achieve distributed sensing of various forms of deformations [108–118]. The assembly of conductive and insulating materials in specific architectures is critical for the realization of such electromechanical devices in fibers. For instance, conductive polymer composite sheets were placed opposite to one another in a bendable cantilever-like polymer structure to detect and localize pressures along the fiber (Fig. 4a) [119]. Under a mechanical load the initially separated conductive domains are brought in contact, acting like a switch in an electrical circuit. The pressure position is determined by measuring the electrical load of this circuit, which depends linearly on the distance from the contact point to the interrogated fiber end. The realization of such pressure sensing capability highlighted here results from the intrinsic flexibility of polymer materials. Furthermore, there has been growing interest in the development of stretchable or soft multimaterial fibers, which is heavily motivated by the excit-

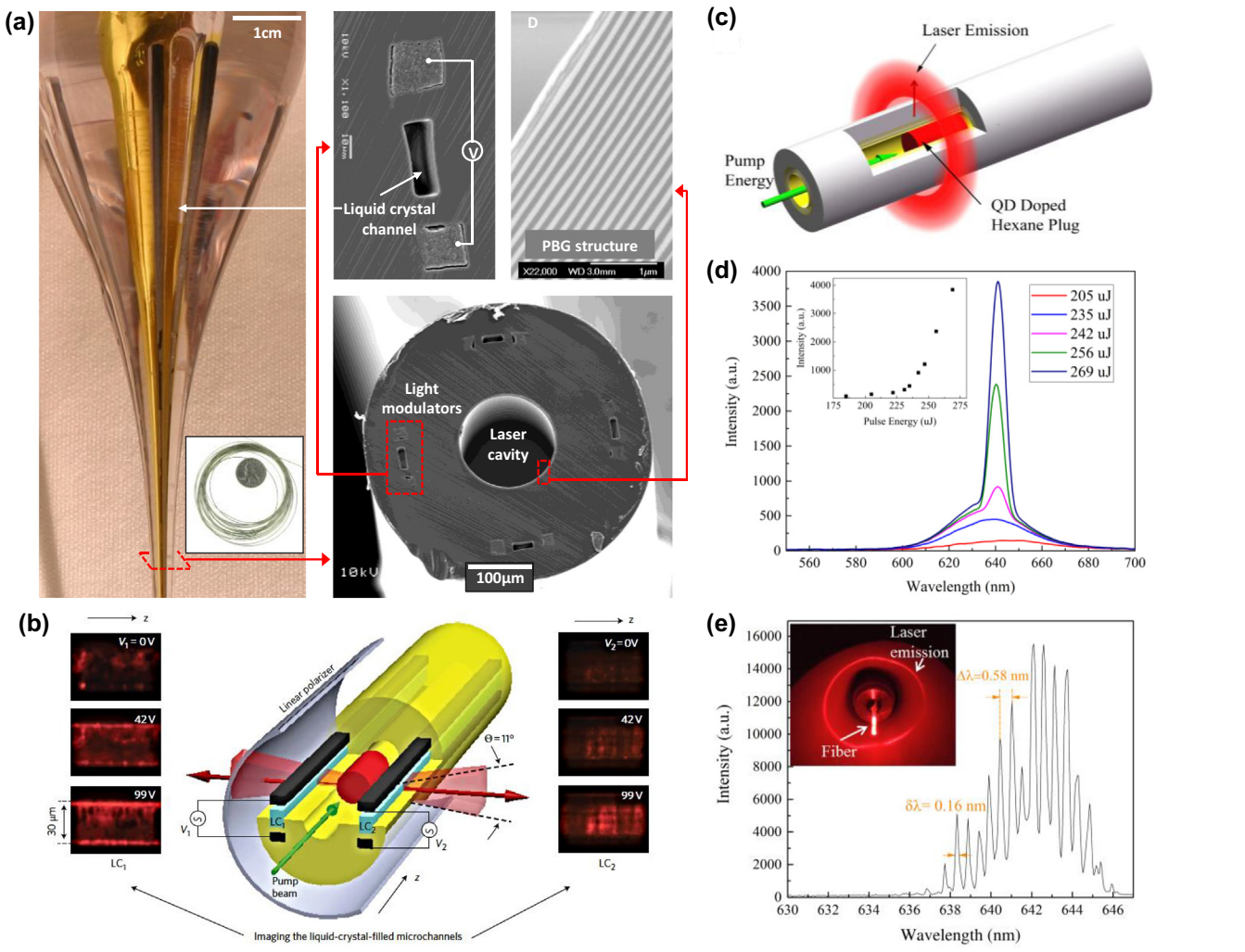

FIGURE 3

(a) Left: Photograph of the drawn preform. Inset: several meters of fiber coiled around a US quarter. Right: SEM image of the multimaterial fiber device (scale bar, 100 μm). The fiber core is surrounded by four light modulators. (b) Schematic of the fiber device depicting the simultaneous control of two oppositely facing liquid–crystal filled microchannels, labelled LC_1 and LC_2. Light blue strips correspond to liquid–crystal-filled microchannels and black strips to in-fiber electrodes. V_1 and V_2 are the voltages applied to the electrode pairs that flank LC_1 and LC_2, respectively. The light intensity passing through LC_1 (LC_2) does not change as a function of the voltage V_2 (V_1), demonstrating the independent control available in each direction. Adapted with permission [57]. Copyright 2012 Nature Publishing Group. (c) Scheme of the laser emission. (d) Spectra of radial emission from the laser cavity collected under different pump pulse energies, and (inset) the dependence of the peak intensity on the pulse energy. (e) High resolution spectrum of the radially emitted QD fiber laser collected at pump energy above the lasing threshold, and (inset) the wavefront of the laser emission in the far field. Reprinted with permission from [99]. Copyright 2016 American Chemical Society.

ing opportunities of electronics that show the ability to conform to the human skin, biological tissue, soft robotics and textiles. Multimaterial electronic fibers that can retain their complex functionalities while bearing different deformation hold important applications in the field of electronic skins, artificial muscles, implantable medical devices and smart textiles. However, thermal drawing of stretchable or soft fibers remained a long-term challenge due to the poor understanding of the rheological properties of materials. Recently, Qu et al discover that the thermal flow in the viscous regime at high viscosities of a thermally-drawn material can be defined as a temperature window where loss modulus decreases slowly with temperature, crossing over elastic modulus that rapidly decreases. Based on this simple criterion, superelastic stretchable fibers constituted of thermally drawn thermoplastic elastomers are developed [61,120–121]. The vast deformations that this material class can elastically undergo is exploited to develop fibers with fully enclosed composite electrodes, which enabled the discrimination of compressive and shear loading (Fig. 4b). In this work, the integration of dynamically responsive liquid metal channels is also explored to extend the functionality of fiber-based devices, such as the quantification of transverse pressure magnitude as well as fiber elongation (Fig. 4b, c). Complex applications using these fibers in smart textiles and robotics are also demonstrated. The low elastic moduli of these types of fibers make them ideal candidates for implantation in spinal cord for dissecting neuron behavior, as we elaborate in Section "Multimaterial multifunctional fibers for neural interfacing". Besides direct thermal drawing of electrodes

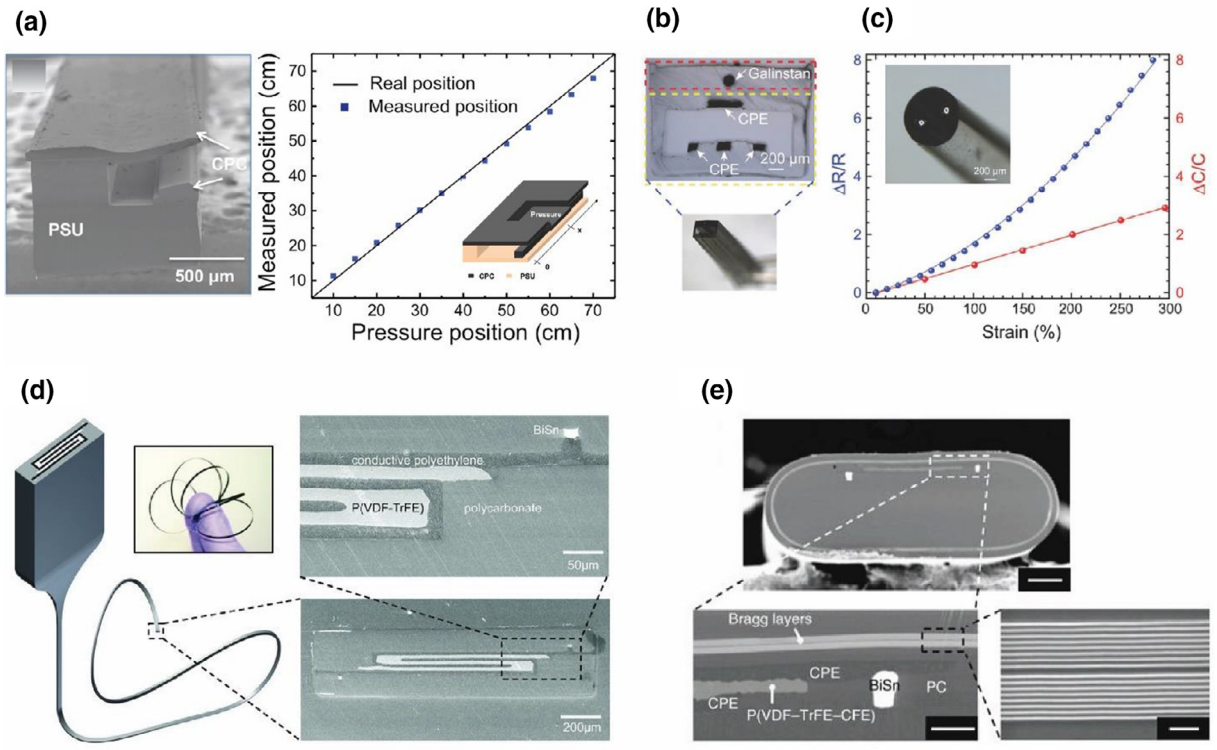

FIGURE 4

(a) Electromechanical fiber for detection and localization of pressures based on cPC electrodes in cantilever-like PSU structure [119]. Reprinted with permission from structure [119]. Copyright 2017, IOP Publishing. (b) Deformable thermoplastic elastomer fiber with a liquid metal channel and four cPE electrodes for the quantification and localization of pressures and the discrimination between compressive and shear loading [61]. Reprinted with permission from [61]. Copyright 2018, Wiley-VCH. (c) Stretchable fiber with liquid metal channels for sensing large strains through changes in resistance or capacitance. Reprinted with permission from [61]. Copyright 2018, Wiley-VCH. (d) Fiber based on the piezoelectric P(VDF-TrFE) contacted by interdigitated cPE electrodes for acoustic emission and reception [128]. Reprinted with permission from [128]. Copyright 2012, Wiley-VCH. (e) Fiber with electrostrictive domain consisting of P(VDF–TrFE–CFE) and cPE electrodes for electromechanical actuation and modulation of integrated Fabry–Pérot cavity [62]. Reprinted with permission from [62]. Copyright 2017, Springer Nature.

within elastomers for making stretchable or soft fibers, other typical technology include patterning liquid metal fibers based on lithography, injection, additive and subtractive methods [122–123], microfluidics-based multicore-shell fiber printing [124], and various coating, deposition, physical wrapping and twisting of functional materials [125–127].

Fibers for energy conversion

The integration of polymers with distinguished dielectric properties has also been investigated in thermally drawn fibers. Copolymers of the piezoelectric poly(vinylidene fluoride) [P(VDF-TrFE)] have opened the door to a novel generation of fiber-based acoustic transducers that can be used both in emission and reception mode over frequency ranges spanning from Hertz to Megahertz. [59]. The challenges that the thermal drawing process poses could be overcome with this material, because it can be confined in its low-viscosity state by highly viscous composite electrodes, and it subsequently crystallizes directly into its ferroelectric phase without necessitating any mechanical stress. The transducer performance could be improved through targeted changes in the design of the fiber architecture, including the maximization of the active surface area through the use of interdigitated electrodes (Fig. 4d) [128]. The benefit of imparting piezoelectric functionality to fibers becomes apparent when considering the collective effect of fiber arrays, which enable coherent interference and beam steering as a transmitter [128] and acoustic positioning as a receiver [129].

Fiber-shaped energy harvesting devices exhibit unique advantages in portable and wearable electronic systems [130]. Among them, fiber-shaped dye-sensitized solar cells (FDSSCs) have attracted great attention recently due to the high efficiency, lightweight and low-cost. Benefiting from the optimization of materials and fabrication techniques, the textiles woven by FDSSCs are capable of exhibiting comparable photovoltaic performances with the planar solar cells [131]. The developed FDSSCs are mainly based on nanostructured TiO_2, which exhibit high efficiency and good flexibility [132,133]. Another class of examples is mechanical energy harvesters, including piezoelectric nanogenerators (PENGs) and triboelectric nanogenerators (TENGs). While PENGs utilize piezoelectric effect to convert the mechanical energy into electricity, TENGs harvest various types of mechanical stimuli ranging from vibration, wind, human motions, to water wave, depending on the coupling effects of contact-electrification and electrostatic induction [109]. Due to the wide choice of materials and ease of fabrication, such nanogenerators with specific features have been designed and fabricated for applications in wearable electronics, sensing, motion tracking, safety monitoring and human-interactive interfaces [134,135]. Despite these advances, the output performance of the fiber-based generators is still much inferior to the planar

architectures. Therefore, further research is still required to improve the outputs of the fiber generators, while maintaining the unique mechanical advantages of fiber structures.

Fiber actuation

Beyond acoustic transduction, a poly(vinylidene fluoride) derivative [P(VDF–TrFE–CFE)] was employed to establish electromechanical actuation in fibers [62]. By sandwiching such a electrostrictive layer between polymer composite electrodes and placing the construct off-axis, the resulting fiber could be made to bend under electrical stimulation (Fig. 4e). By applying 200 V DC, a fiber with 3.5 cm free standing length could be deflected transversely up to 80 μm. Applications of such shape-changing fibers are foreseeable in various domains, including robotics and surgery.

Microfluidic fibers

While being versatile, conventional planar microfluidic systems are still restricted in size by silicon wafers, and in the limited control over geometry and positioning of microchannels. Its inherent scalability and design freedom over the cross-sectional geometry make thermal drawing an intriguing alternative as a microfluidics platform [136]. Indeed, microfluidic fibers with complex microchannel shapes, including crosses and stars, are fabricated to study the inertial particle focusing behavior in the channels [63]. Moreover, through thermal drawing additional functional elements can be integrated in the fibers and coupled with the microchannels. For instance, by incorporating conductive materials along the surface of a crescent-shaped channel, an optimized inertial-dielectrophoretic particle manipulation fiber for high-throughput cell separation is accomplished (Fig. 5a) [63]. Another appealing example is a fiber-based micro-flowrate sensor, which incorporates a hollow microfluidic channel and an adjacent temperature-sensitive CPE film within a polymeric insulator matrix (Fig. 5b). It exhibits higher sensitivity, smaller temperature rise and pressure drop compared to standard MEMS sensors [137]. The creation of these fiber-based microfluidic devices has opened new possibilities for the application of lab-in-fiber technologies in chemical, biochemical and medical fields.

Capacitive fibers

The integration of electrically conductive electrodes with dielectric materials in fibers allows the construction of various capaci-

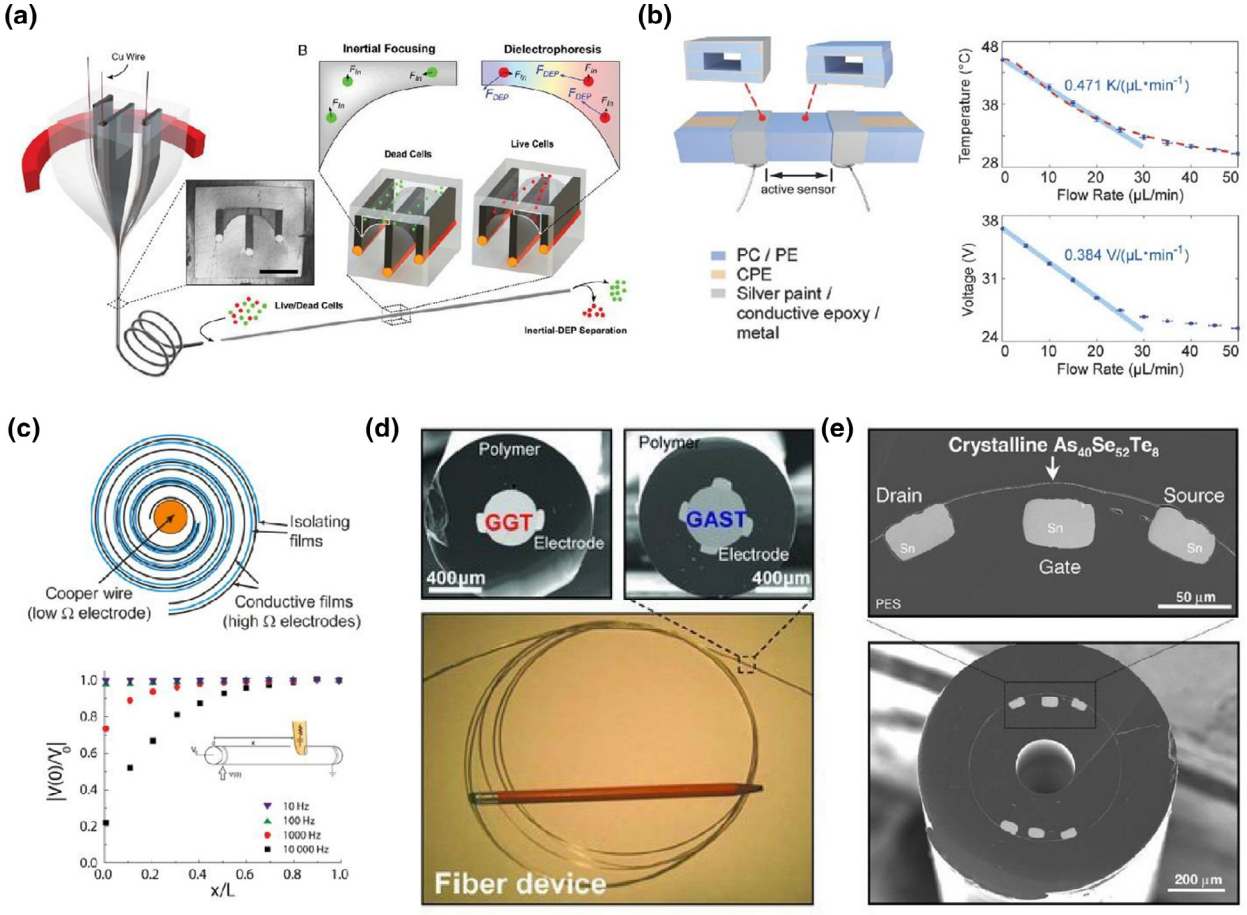

FIGURE 5

(a) Inertial-dielectrophoretic particle manipulation fiber as a microfluidics system for high-throughput cell separation [63]. Copyright 2018, National Academy of Sciences. (b) Fiber-based thermal flow sensor with a linear temperature and voltage responses to various flow rates [137]. Copyright 2018, Wiley-VCH. (c) Detection of touch with a swiss-roll-like capacitive fiber [139]. Copyright 2012, IOP Publishing. (d) Fibers with phase-change high tellurium-content chalcogenide glass and metallic electrodes for ovonic memory switch [60]. Copyright 2011, Wiley-VCH. (e) Fiber field-effect device with Sn electrodes and in situ crystallized $As_{40}Se_{52}Te_8$ film [46]. Copyright 2010, Wiley-VCH.

tive fiber devices. A particularly promising candidate as a dielectric material is poly(vinylidene fluoride) (PVDF), because its high dielectric constant results in a high capacitance in devices. For instance, all-in-fiber capacitors with a low-loss capacitive behavior of up to 20 kHz were demonstrated, by sandwiching a PVDF thin film between CPE electrodes. [138]. Optimizing the design of the fiber architecture by folding wide PVDF film shows increased capacitances in fibers up to 47 nF m^{-1}. A further increase in capacitance of 100 nF m^{-1} is achieved through a swiss-roll like structure, where two dielectric and two conductive polymer layers are rolled up together [139]. The sub-millimeter thick fiber containing 30 layers could additionally function as a 1D touch sensor (Fig. 5c). By integrating an array of the capacitive fibers into a woven textile, a touchpad sensor without inter-channel crosstalk is also demonstrated.

Ovonic memory-switching fibers and field-effect transistor fibers

Materials that exhibit reversible amorphous/crystalline phase transitions under applied electric fields are extensively used in modern data storage media. The ideal trade-off between the high thermal stability required for processing and the low stability needed for phase change is found for high tellurium-content glasses ($Ga_{10}Ge_{15}Te_{75}$ and $Ge_{22}As_{18}Se_{15}Te_{45}$) and ovonic memory-switching fibers are realized (Fig. 5d) [60]. An applied electric field generated by adjacent metallic electrodes in the fiber modulates the electronic structure of the semiconductor domain, leading to a reversible switching between a high resistance (OFF) and a low resistance state with a difference of four orders of magnitude. Beyond this, the in situ phase transition of a glassy chalcogenide compound ($As_{40}Se_{52}Te_8$) from its amorphous to crystalline state allows the construction of a fiber-based p-channel field-effect device (Fig. 5e) [46]. It is envisioned that the processibility of such materials could implement complex circuits along kilometer-long fibers and further contribute to crossbar fabric-array flexible electronic devices.

Fibers thermal sensing, positioning and cooling

Thermal sensors reveal important information about the dynamics of many chemical, physical and biological phenomena and are one of the most frequently employed sensors for industrial processing, medical diagnosis, and military defense. Typical thermal sensors are based on thermistors, thermoelectrics or IR radiation. However, it is still challenging to develop a flexible thermal sensor to detect a thermal excitation over a large area while considering the irregularity of the monitored surface, spatial constraints, or cost.

The first attempt of multimaterial thermal sensing fiber was based on $Ge_{17}As_{23}Se_{14}Te_{46}$ (GAST) with metallic electrodes made of the alloy $Sn_{96}Ag_4$ [58], as shown in Fig. 6a. Intimate contacts are formed at the glass/metal interfaces. The fibers are flexible, lightweight, and protected (electrically and chemically) from environmental effects. When the metal electrodes are connected to an external circuit, a functional thermal sensing device is obtained. The fabricated fibers are arranged on a grid structure while embedded in a fabric, forming an 8 × 8 array with a separation distance of 1 cm between neighboring fibers. Two situations are presented: A) localized heating by the touch of a finger and B) cooling with an ice cube, as shown in Fig. 6a. These results confirm the capability of localizing the source of a thermal excitation to within the resolution of the fiber placement in the array.

The second attempt was based on the Cu-As-Te-Se system, as these semiconducting glasses possess a large Seebeck coefficient ranging from 400 to 1100 μV/K, despite a low TE figure of merit, and show great potential for the application of thermal sensing [140–141]. To increase the contact area between the heat source and TE fiber and reduce the heat loss between the heat source and semiconducting glass core, rectangular-shaped PEI blocks are selected. Fig. 6b shows a photograph of the resulting TE fiber and an optical microscope image of the cross-section. For thermal sensing, large Seebeck coefficients are needed to guarantee the high sensitivity and accuracy of the thermal sensor, where a fast and large voltage generation occurs from a minimal temperature change. Although a single TE fiber can sense temperature with a fixed location or position of the thermal source with a fixed temperature by the output voltage, it is difficult to obtain both the temperature and the location of the thermal source. To address this challenge, a flexible thermal sensor network is constructed based on a 3 × 3 TE fiber array woven into a flexible textile as a prototype to obtain spatially resolved thermal information, including both thermal sensing and positioning, as shown in Fig. 6c. These results confirm the capability of the TE fiber array for ultra-flexible and large-area detection, localization and monitoring of the thermal source with a high spatial resolution of the temperature.

The third attempt is based on crystalline TE materials [64]. Both p-type $Bi_{0.5}Sb_{1.5}Te_3$ and n-type Bi_2Se_3 are used as the TE fiber cores, and the borosilicate glass tube is the best choice for the cladding material. Two types of thermoelectric fiber generators covered on different curved surfaces have been demonstrated to provide a mW/cm^2-level output power density, which is among the highest levels for flexible and wearable thermoelectric devices achieved so far. Additionally, a wearable two-dimensional active-cooling textile has been assembled using these thermoelectric fibers, and a maximum cooling of 5 °C has been achieved, as shown in Fig. 6d. These fibers can be further woven into fabrics, which makes them particularly suitable for applications including green buildings, industrial energy management, wearable electronics, smart fabrics, and large-area sustainable energy generation systems.

Scintillating fibers for radiation detection

Radiation detection is critical for various applications, such as nuclear monitoring, geophysical exploration, radiotherapy, and high-energy physics. The scintillating fibers are believed to provide unique advantages for these opportunities. Firstly, these fibers can be easily coupled with flexible transmission fibers, allowing for performing in situ radiation measurement in remote and real-time mode [142]. Secondly, various functional units can be hybridized into scintillating fibers forming multimaterial fibers with complex structure, which has been demonstrated to be favorable for high-energy photon harvesting [143–145]. A typical example is that the phase transition of Gd-Ta-O triggered in a scintillating fiber creates efficient energy-harvesting pathways, resulting in the more than 5-fold improvement in the detection

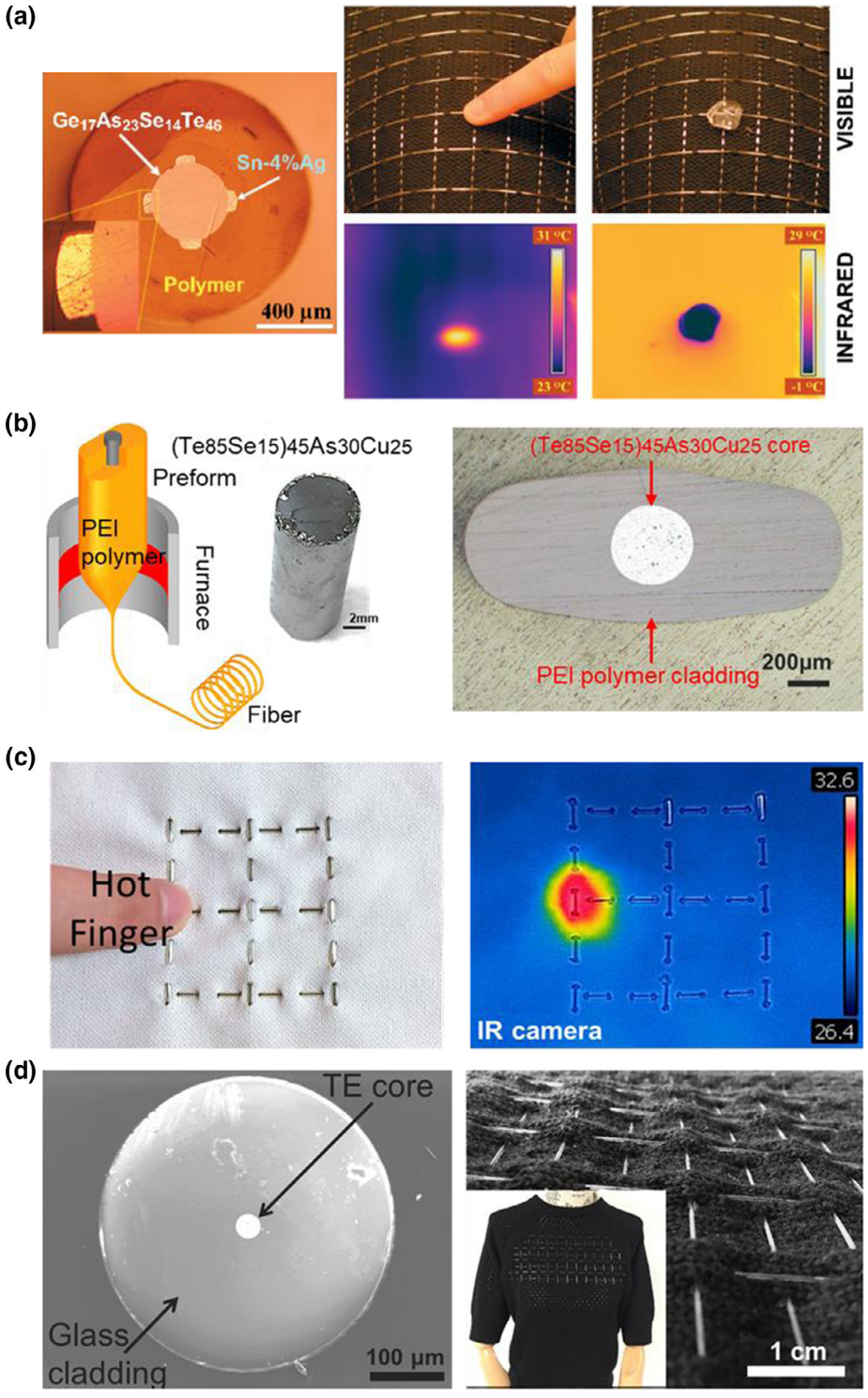

FIGURE 6

(a) Images of the fiber cross section and an 8 × 8 array to detect the localized heating by the touch of a finger and cooling with an ice cube. Reprinted with permission from [58]. Copyright 2006 Wiley. (b) A thermoelectric fiber is fabricated by thermally codrawing a macroscopic preform containing a semiconducting glass core and a polymer cladding. (c) A two-dimensional 3x3 fiber array is woven into a textile to simultaneously detect the temperature distribution and the position of heat/cold source with the spatial resolution of millimeter. Reprinted with permission from [141]. Copyright 2019 American Chemical Society. (d) Crystalline thermoelectric fiber with borosilicate glass cladding. a wearable two-dimensional active-cooling textile is assembled using these thermoelectric fibers and a maximum cooling of 5 °C has been achieved. Reprinted with permission from [64]. Copyright 2017 Elsevier.

performance [145]. Furthermore, the constructed composite fibers can also be regularly arranged into a special fiber array detector, in which each fiber can be regarded as an individual pixel. This type of unique detector is expected to be able to study the spatial distribution of radiation with suppressed signal crosstalk.

Strain-programmable fibers for artificial muscle

Artificial muscles capable of converting electrical, chemical or thermal energy into mechanical deformation have great promise for applications in robotics, haptics and prosthetics. Among the various actuators, polymer and composite alternatives provide the attributes of high power-to-mass ratios and strains [146,147]. However, producing these structures with fast temporal responsiveness and tunable dimensions remains a big challenge. One of the intriguing characteristics of thermal drawing is that it delivers adjustable dimension depending on the scale-down ratio. Very recently, Kanik et al. exploited thermal drawing of a polymeric bimorph structure consisting of an elastomer and a regular thermoplastic polymer for the production of artificial muscle fibers at scale with dimensions spanning three orders of magnitude [65]. As shown in Fig. 7a, the fiber is composed of elastic COCe and high-density PE encapsulated within a PMMA cladding. A first draw generates fibers with feature sizes scaling between a few millimeters and tens of micrometers. Stacking the first-drawn fibers in a second preform and drawing it reduces the feature size to a few micrometers. The poor adhesion between the cladding the bimorph structure allows for direct peel-off of the sacrificial PMMA cladding and straightforward use of the bimorph structure (Fig. 7b). Upon mechanical drawing these bimorph fibers at strains of 50–1300% at room temperature, the PE undergoes plastic deformation while the COCe is elastically deformed. When releasing the fiber, the elastomeric COCe tends to contract to its original shape, and resulting stress induces the formation of tendril-like springs (Fig. 7c). A wide range of fiber springs with varied cross-sectional dimensions are obtained via this approach, as shown in Fig. 7d. The difference of the thermal expansion coefficient between the COCe and PE is as large as fivefold, enabling rapid reversible and repeatable actuation upon external thermal stimulation. It's reported that a single 5-cm-long fiber with a cross- sectional area of 300 μm by 470 μm could lift a 1-g weight by a strain of 12% in response to a thermal stimulus of temperature change of 10 °C (Fig. 7e). Inspired by human arms, the authors print an artificial limb and use the fiber muscle to connect the forearm and the humerus for the demonstration of fiber-based artificial muscle. As shown in Fig. 7f, the miniature arm is able to lift a 1-g dumbbell for multiple cycles. The scalable feature size of the fiber artificial muscles with unique strength and responsiveness demonstrated here might open a novel path to applications in robotics and prosthetics.

Optoelectronic fibers

The integration of conducting and semiconducting domains forms optoelectronic devices, which are traditionally produced using standard wafer-based processes. Although the resulting devices are small and low-cost, they are restricted to planar geometries and mechanically rigid substrates. The unique combination of metals, insulators and semiconductors into one-dimensional fibers enables optoelectronic functionalities over large-area, flexible, soft and stretchable substrates. In this section, we will review optoelectronic fibers for photosensing, lensless imaging, chemical sensing and optical communications.

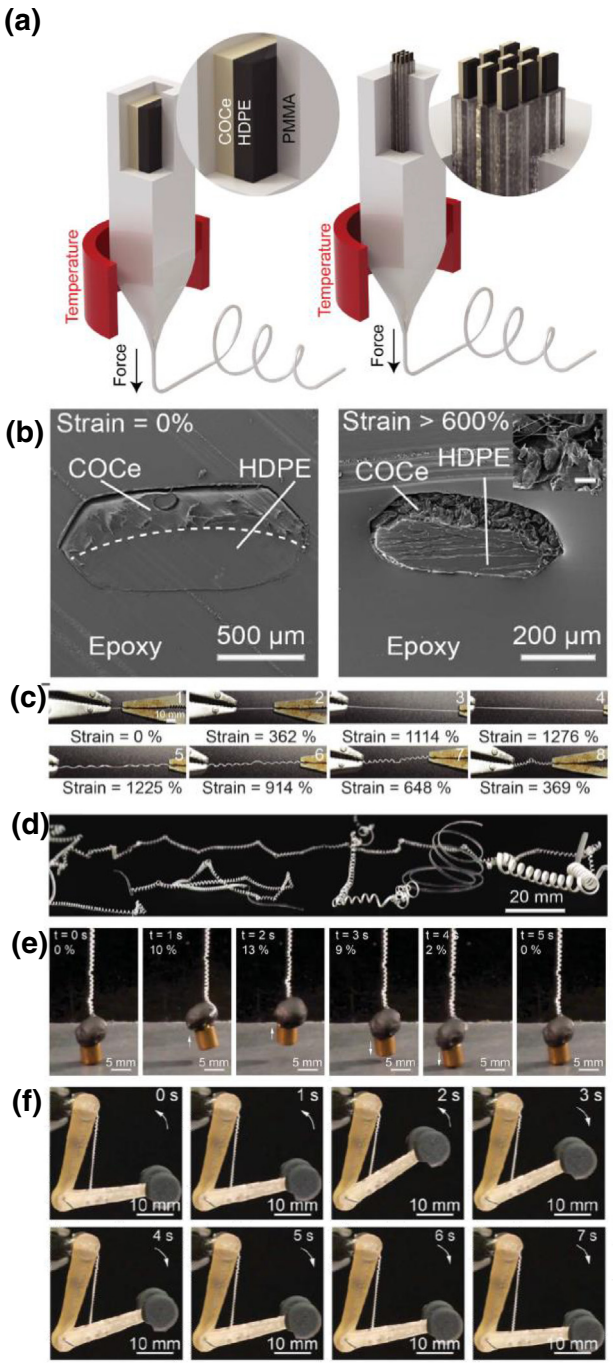

FIGURE 7

(a) Fabrication method for artificial muscle fibers. (b) Cross-sectional SEM images of the fiber before/after cold drawing. (c) Cold drawing for obtaining a spring actuator. (d) Photograph of artificial muscles. (e) Photographs showing the process of lifting a weight with a fiber. (f) A photographic time series of the artificial limb lifting a 1-g load. Reproduced with permission [65]. Copyright 2019, AAAS.

Optoelectronic fibers for photosensing

The first metal–semiconductor-insulator optoelectronic multimaterial fiber is created in 2004 [53]. Chalcogenide glasses are chosen because of their unique photodetecting capability in the visible and IR ranges, tunable optoelectronic properties

depending on their composition and low-temperature processing windows compatible with those of polymers [148–150]. As shown in Fig. 8a, this fiber consists of an amorphous chalcogenide glass core ($As_{40}Se_{50}Te_{10}Sn_5$) that interfaces by four metallic electrodes (Sn) that run along the fiber length and are encapsulated by a transparent polymer cladding. External light impinging at any position of the fiber produces a photocurrent measured by connecting the metallic electrodes to external circuits. Note that the spectral range of the photodetection for this chalcogenide glass is broad. Surrounding the photodetecting domain with PBG structure only allows the desired wavelength to target the core, enabling narrowband photodetectors (Fig. 8a) [53]. One important figure of merit for characterizing the performance of photodetectors is the sensitivity defined by the photocurrent divided by the noise current. For a fiber configuration where the semiconductor is cylindrical, the photosensitivity is inversely proportional to the core dimeter. Thus, tuning the geometry and structure of the core is expected to change the photodetection. Indeed, Sorin et al. demonstrated that the sensitivity of a thin-film configuration (Fig. 8b) is significantly larger than a solid-core fiber [151]. However, these photodetecting devices could not provide any information about the spatial localization of a single incident optical beam along the fiber. It is then demonstrated that the simultaneous localization of three points of illumination can be achieved through the construction of a convex electrical potential along the axis of a single fiber [152]. Furthermore, the wavelength and incident angle can be discriminated by a highly complex fiber that incorporated eight photodetecting devices with feature sizes down to 100 nm (Fig. 8c) [56].

The semiconductor core in the first-generation optoelectronic fibers is amorphous. A disordered atomic structure is detrimental to the electronic and optoelectronic properties of the devices. Tremendous efforts have been made to fabricate high-performance fiber optoelectronics. Indeed, photodetectors with ultrahigh sensitivity, response speed and responsivity have unique applications in in vivo imaging, military monitoring, and the dissection of neural activities in the brain. Alteration of the atomic structure of the semiconductors in these optoelectronic fibers is always performed post-drawing using different annealing strategies. The most straightforward method is to thermally anneal the amorphous core at a high temperature above the glass transition temperature [47], leading to a solid phase transformation from an amorphous core to crystalline semiconductors. Despite the improvement in electrical properties, the highly dense nanograins in the resulting polycrystalline semiconductors with an ultralarge volume of grain boundaries severely impair the optoelectronic performance of the devices [153]. The second strategy exploits laser heating, where the amount of energy that can be precisely controlled can be delivered into a confined region of the semiconductors. Tuning the laser energy, laser wavelength and on/off rate can control the crystallinity, grain size, crystallographic orientation and even the elemental segregation [48]. It is demonstrated that a laser

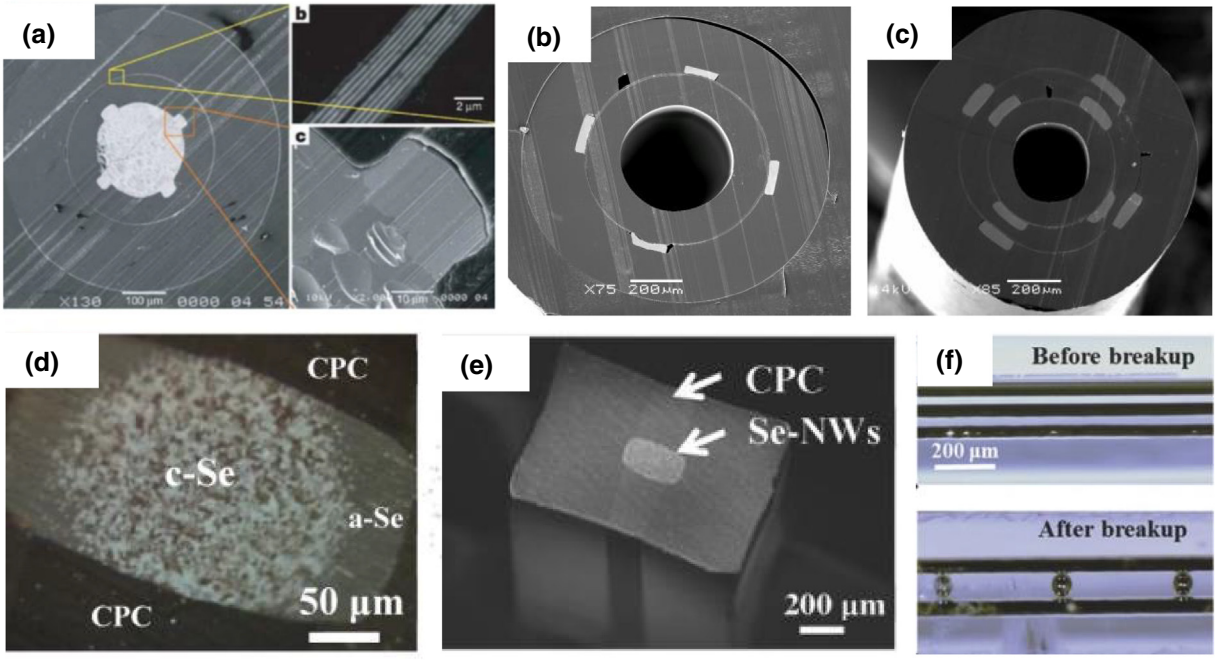

FIGURE 8

(a) An optoelectronic fiber composed of an amorphous chalcogenide glass core ($As_{40}Se_{50}Te_{10}Sn_5$) interfaced by four metallic electrodes (Sn). The optoelectronic core is surrounded by a PBG fiber forming a narrow-band photodetecting system. Reproduced with permission [53]. Copyright 2004, Nature Publishing Group. (b) An optoelectronic fiber with a thin-film configuration. Reproduced with permission [151]. Copyright 2007, Wiley-VCH. (c) An optoelectronic fiber with eight photodetectors. Reproduced with permission [56]. Copyright 2009, American Chemical Society. (d) An optical micrograph of a Se-core optoelectronic fiber that was annealed via laser heat treatment. Reproduced with permission [153]. Copyright 2017, OSA. (e) A Se nanowire-based optoelectronic fiber. Reproduced with permission [50]. Copyright 2017, Wiley-VCH. (f) Selective break-up in-fiber semiconductor core. Reproduced with permission [70]. Copyright 2016, Wiley-VCH.

annealing treatment led to ultralarge grain formation in a Se-core optoelectronic fiber (Fig. 8d) [153]. The resulting fiber showed drastically improved photoresponsivity and photosensitivity several orders of magnitude higher than that in a fiber annealed using conventional heat treatment. The third approach relies on a phase transformation in chemical solutions in which the solvent can modulate the surface energy of crystal planes when crystals are growing from nuclei [50,154,155]. Fig. 8e shows such a novel method for integrating high-quality monocrystalline semiconducting nanowires within optoelectronic fibers. The fiber devices exhibit unprecedented optoelectronic performance, demonstrated by their high photoresponsivity and photosensitivity, low dark current, low noise-equivalent power and ultrafast response speed, which are on par with many wafer-based devices. Besides photosensing, the integration of nanowires into fibers opens a breadth of impressive applications in flexible electronics [156], novel laser emission [157], solar cells [158].

The second strategy for the fabrication of optoelectronic fibers is thermal drawing of semiconductors with high melting points, such as Si, Ge, SiGe and GaSb, within the glass platform [159–163]. The initial motivation for making such semiconductor-core optical fibers is to extend the accessible wavelength range beyond the telecommunication wavelength range realized by traditional optical fibers. However, forming highly efficient electronic junctions by interfacing these semiconductors with electrodes remains technologically challenging because both crystalline electrodes and semiconductors are in molten states at such high temperatures. Wei et al. developed an innovative method to overcome this challenge by leveraging the Plateau-Rayleigh instability in the fiber platform [70]. As shown in Fig. 8f, a heat source is exploited to selectively break the semiconductor core into spheres, during which the spheres push the soft silica aside and directly contact the electrodes that remain intact during the heat treatment. This is a versatile approach for creating a variety of semiconducting functionalities within fibers, since the elements can be independently addressed. For example, another work shows that this principle can be applied in a polymer platform where the heat treatment only allowed the amorphous chalcogenide glass (As_2Se_5) to break into discrete spheres while keeping the conductive domains (CPE) unchanged [164], forming $\sim 10^4$ self-assembled, electrically contacted and entirely packaged discrete spherical devices per meter of fiber.

Optoelectronic fibers for lensless imaging

As described in the previous section, a single optoelectronic fiber can only discriminate three points of the incident illumination. Constructing a closed-surface sphere using these optoelectronic fibers [55], on the other hand, provides directional detection over a full 4π steradians. The intensity distribution an also be measured by constructing a set of parallel photodetecting fibers into a planar array to form a 'parallel projection' of the incident intensity distribution combined with a tomographic algorithm. These projections can be obtained by different strategies, such as directly rotating the fiber array, using different arrays rotated with respect to each other and rotating the object being imaged. Furthermore, both the amplitude and phase of an optical illumination were obtained from a dual-plane construct. When an object is illuminated with a laser beam, the propagating diffracted field amplitude can be measured at two different locations using these two fiber webs. A phase-retrieval algorithm is then used to obtain back-propagated images in the direction receding from the fiber webs towards the object. Non-interferometric lensless imaging using two fiber webs is thus realized.

Another example is fluorescence imaging, which only exploits a hybrid fiber integrating an optical fiber and a couple of photodetectors [50]. The incident light is guided along the optical fiber and illuminates a fluorescent material that emits photons. Due to the excellent photosensitivity of the photodetectors, the emission light is immediately detected by the sensors at the fiber tip. Scanning the fiber along the object and recording the photocurrent intensity distribution enables imaging without a lens. This highly integrated fiber is drastically different from traditional discrete systems where the photodetectors are placed at the distal end of the optical fiber.

Optoelectronic fibers for chemical sensing

Capturing and detecting toxic and hazardous vapors is extremely important. Optoelectronic fibers for chemical sensing have been fabricated based on a chemiluminescent principle. Photoconductive detectors embedded directly in the fiber along the entire fiber length capture emission light anywhere within the hollow core [40]. The resulting electrical signals are immediately recorded by fiber electrodes that intimately interface with the semiconductor ($Se_{97}S_3$). However, the amorphous as-drawn $Se_{97}S_3$ generates a very large noise current, making it difficult to detect a weak illumination from chemiluminescence. The fiber is thus thermally annealed above the glass transition temperature of $Se_{97}S_3$ to induce crystallization, which significantly improves the sensitivity. The detection of trace levels of peroxide vapor down to 10 ppb was achieved, comparable to the detection level of state-of-the-art commercially available systems. The photoconductor can extend hundreds of meters, realizing a new platform for remote and distributed chemical sensing.

Optoelectronic fibers for optical communications

The formation of high-quality heterojunctions requires that two different semiconductors intimately contact each other. The fabrication of semiconducting diodes in multimaterial fibers is a considerable challenge because of the inter-mixing issue as we described before. Although a high-pressure chemical vapor deposition technique with different materials deposited sequentially can produce many unique devices, such as Ohmic junctions, p-n junctions, Schottky junctions, and p-i-n junctions [165–167], the approach is not scalable and the fiber is short. Recently, Prof. Yoel Fink's group at the Massachusetts Institute of Technology developes a revolutionary method for the incorporation of high-performance commercialized semiconducting diodes into functional fibers based on the thermal drawing technique [52]. As shown in Fig. 9a, the prefabricated devices and electrical conductors are incorporated into the polymer-clad preform first. As the preform is thermally drawn, the diodes confined in their pockets flow along the fiber axis, and the electrical conductors are continuously fed into the fibers. The lateral spacing of these conducting wires is gradually reduced in the neck-down region until electrical contact is achieved with these diodes. The authors

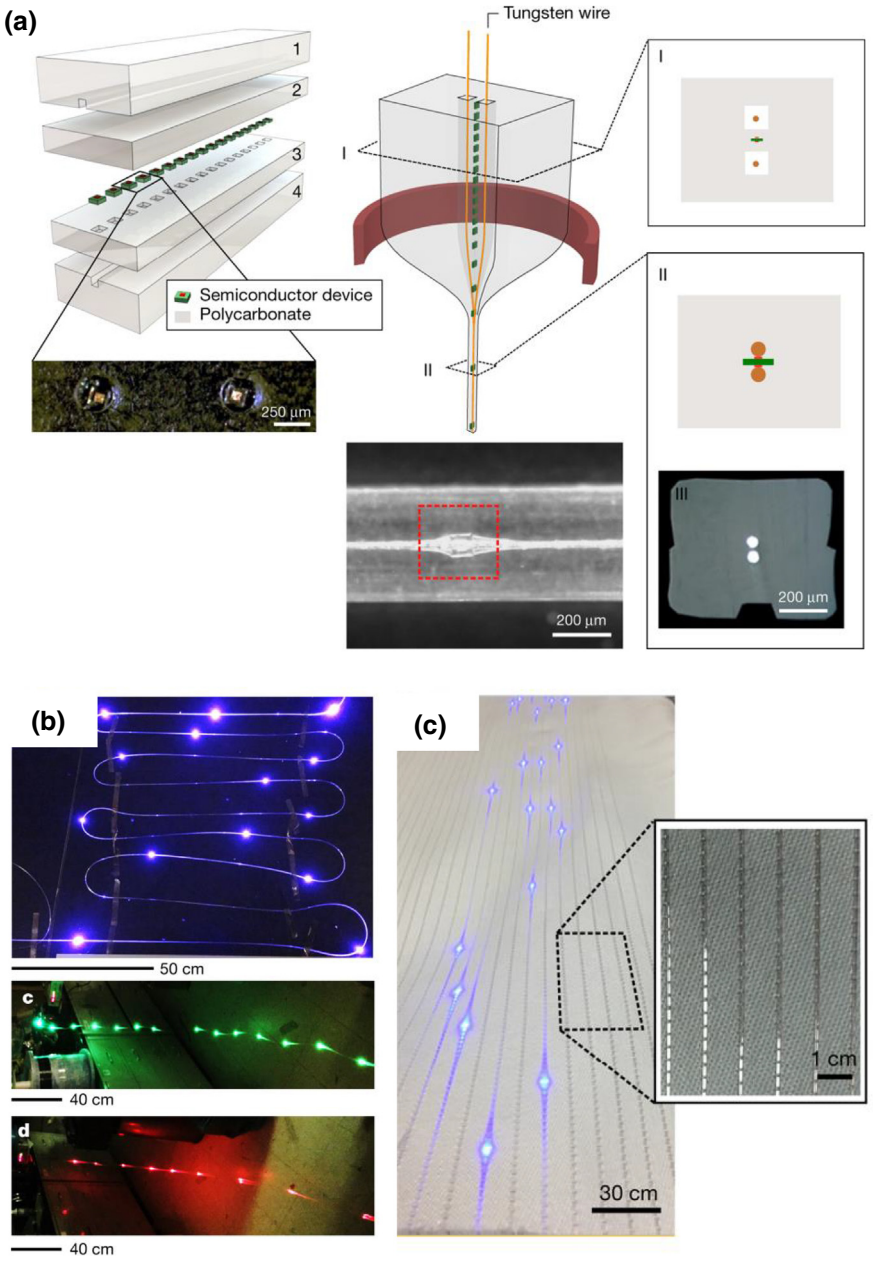

FIGURE 9

(a) Illustration of the preform making, thermal drawing process and fiber architecture. (b) Photographs of light-emitting fibers containing InGaN blue-color, green-color and red-color LEDs. (c) Light-emitting and photodetecting fibers integrated in a fabric. Reproduced with permission [52]. Copyright 2018, Nature Publishing Group.

could successfully incorporate two types of devices into the fibers: light-emitting and photodetecting p-i-n diodes. Both fibers are woven into a separate textile polyester fabric using a conventional industrial loom, and they are fully functional throughout ten machine-wash cycles (Fig. 9b and c). The integration of high-speed optical transmitters and receivers into fabrics has compelling applications. They demonstrate a three-megahertz bi-directional optical communication link using two fabrics containing receiver-emitter fibers. Heart rate measurements with diodes are also realized. This work demonstrates a new paradigm for the integration of highly sophisticated functionalities into fibers and textiles. We envision that the density of devices and complexity of the functionality will significantly increase in the future.

Multimaterial multifunctional fibers for neural interfacing

Fibers share a lot of commonalities with neurons. The prospect of creating a connection between the neuronal and the electronic communication networks could lead to a new class of neuron-integrated electronic devices, and holds great promise for both fundamental science and medical device applications. Over the past decades, significant progress has been made in fiber-based

neural interfaces. Based on the interfacing method, the fiber devices can be categorized into optical, electrical, chemical, scaffolding fibers, and the ones combining multiple modalities (see Fig. 10).

Optical interface

With the emergence of optogenetic tools, conventional silica optical fibers have been inserted into animal brains and spinal cords for modulating the activities of neural assembles [168–172] (Fig. 10a). It provides a powerful tool for modulating the neuronal activity and for deciphering the neural circuitry underlying behavior with immediate, precise control. It also offers potential new strategy for treating various neurological diseases [173–179].

Two other powerful techniques enabled by optical fiber-based interfaces are fiber photometry [180–182] (Fig. 10b) and *in vivo* fluorescence imaging [183–185], both detecting the activities of fluorescence expressing cells in the brain. Due to the low loss and deep tissue penetration of optical fibers, they are well-suited for detecting the fluorescence dynamics *in vivo*. The limitation of photometry is the lack of single-cell resolution due to the convoluted signals obtained from photon counting. Fibered

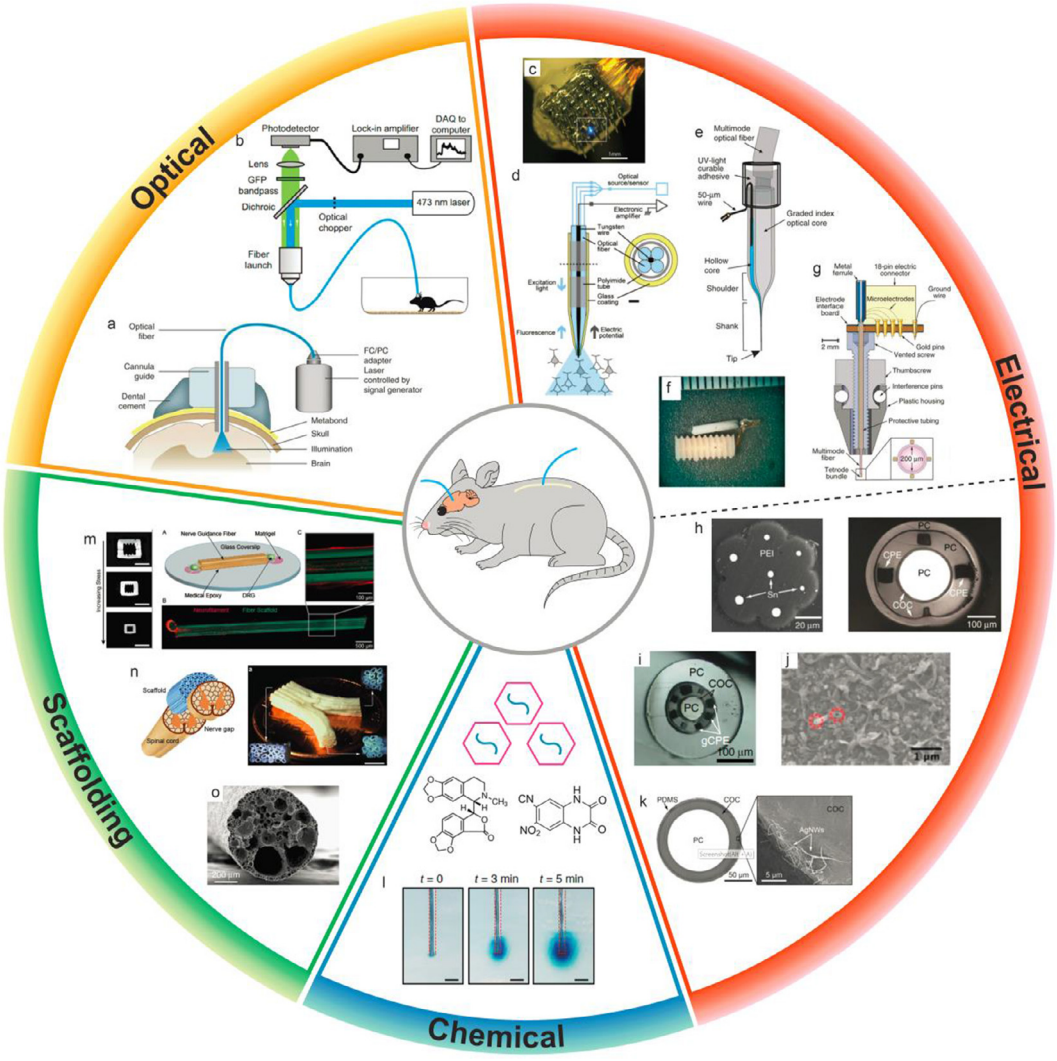

FIGURE 10

Fiber-based neural interfaces. (a) A schematic of *in vivo* optogenetic stimulation setup [172] Copyright 2010, Springer Nature. (b) A schematic of fiber photometry setup [181] Copyright 2014, Elsevier. (c) Optical fiber outfitted to microelectrode arrays with conductive coating [189] Copyright 2012, IOP Publishing. (d) Four optical fibers with one tungsten wire in the center for optogenetic investigation in deep brain structures [186] Copyright 2012, Elsevier. (e) A microprobe with electrolyte as electrical recording interface with single cell resolution [193] Copyright 2011, Springer Nature. (f) Optical fiber with stainless steel microwires for closed-loop optogenetic intervention [177] Copyright 2013, Springer Nature. (g) Optical fiber with four tetrodes attached to freely moving animals [187] Copyright 2011, Springer Nature. (h) Multimaterial multifunctional fiber-based neural probe [38] Copyright 2015, Springer Nature. (i) Fiber probe with graphite-loaded CPE electrode for one-step optogenetics [66] Copyright 2017, Springer Nature. (j) CNF-CPE composite fiber electrode with improved electrical performance [203] Copyright 2017, American Chemical Society. (k) Stretchable fiber with dip-coated silver nanowires for optogenetic stimulation and recording in the spinal cord [205] Copyright 2017, AAAS. (l) Drug delivery demonstration of a multifunctional fiber [66] Copyright 2017, Springer Nature. (m) Fiber scaffolds with microgrooves for nerve guidance [209] Copyright 2015, Elsevier. (n) Porous fiber generated by salt-leaching, and 3D printed to a centimeter scale [210] Copyright 2019, Wiley-VCH. (o) Porous fiber produced by phase separation [73] Copyright 2017, Nature Springer.

fluorescent microscopy (FFM), on the other hand, utilizes fiber bundles to obtain the actual fluorescence image, and can achieve a higher spatial resolution.

Electrical interface

Silica optical fiber with integrated electrodes

Electrical recording is widely used for detecting neural activities due to its high temporal resolution and relatively simple instrumentation. To realize bidirectional communication with neural circuits, several methods have been developed to integrate recording electrodes into conventional optical fibers (Fig. 10c–g). One of the most commonly used methods is manually attaching metal microwires [179,186,187] to optical fibers. Alternatively, conductive gold coating has been applied to optical fibers as electrical interfaces [188–190]. To increase the electrical readout channel counts, optical fibers have been incorporated into existing silicon-based multielectrode devices [189,191]. Besides, an electrolyte solution hosted in a microfluidic channel has been used to record neural activities [192,193]. Recently, Zhao et al. have also attached a flexible nanoelectronic device onto optical fiber surface for multimodal interfacing [194]. To minimize optical connection and tethered cables, μLEDs [195] and laser diode chips [196] have been incorporated into electrical recording devices as alternative ways of delivering light in deep brain.

Multimaterial multifunctional fibers

Although silica optical fibers can deliver light into deep tissues with low losses, the mechanical property mismatch between rigid silica fibers and soft brain tissue can lead to tissue damage and bio-incompatibility [197–199]. Therefore, polymer-based, flexible, and biocompatible waveguides have been actively explored [200–201]. Furthermore, to establish two-way communication with the neural circuits, a multifunctional probe with optical waveguiding and electrical recording capabilities is desired [187,195,202]. The multimaterial fiber drawing method provides an ideal platform for creating these devices (Fig. 10h–k).

The first multimaterial multifunctional fiber-based neural probe was developed by the Anikeeva and Fink groups at MIT [38]. These fibers, fabricated using the multimaterial fiber drawing method, are capable of simultaneous *in vivo* optical stimulation, electrical recording, and drug delivery [38]. Using a two-step fiber drawing process, fiber probes with 7–36 tin electrodes inside a polyetherimide (PEI) cladding were produced. To enable simultaneous optical transmission and electrical recording, PC/COC core/shell structures were used to create the optical waveguides due to their large refractive index difference, and carbon-loaded polyethylene (CPE) was used as the recording electrodes to produce an all-polymer probe. These fibers were implanted into the medial prefrontal cortex of transgenic mice (Thy1-ChR2-YFP). Optically-triggered neural activities were recorded using a single implanted device. These polymer-based fiber probes are much more flexible compared to silica fibers, with a bending stiffness as low as 4–7 N/m. Besides, they are also biocompatible, showing minimal tissue responses after being implanted for three months [38].

Nevertheless, the low electrical conductivity of CPE leads to a poor spatial resolution of the all-polymer probes. To overcome this challenge, many efforts have been made. Carbon nanofibers (CNFs) were introduced into the conventional CPE electrodes. During the thermal drawing process, unidirectional alignment of CNFs was achieved, resulting in drastically increased conductivity along the fiber longitudinal direction. Therefore, the electrode sizes can be reduced significantly without sacrificing the recording signal quality [203]. Similarly, graphite was employed into CPE to increase the electrical conductivity of the electrodes and improve the spatial resolution in a multifunctional fiber probe [66].

Beyond brain interfacing, multimaterial multifunctional fibers are also ideal candidates for stimulating and recording the spinal cord due to the mechanical compliance of these fibers [204]. To further enhance the mechanical performance, stretchable fibers have been developed for simultaneous optical stimulation and electrical recording in the spinal cord [205]. The stretchable waveguide consists of COC elastomer (COCE) and polydimethylsiloxane (PDMS) as the core and cladding, respectively. The electrical interface was created by dip coating conductive silver nanowires (AgNWs) onto the fiber surface. The mesh electrode of AgNWs was more resilient to bending and stretch deformation compared to conventional electrodes.

Chemical interface

Chemical delivery, combined with electrical and optical interfaces, can offer additional control over the neural activities providing insights to the neural circuitry [206,207]. Intracranial drug or viral vector delivery typically utilizes cannulas (metal tubes) or needles. Researchers have also employed fiber-guided cannula as the drug delivery channel [169]. However, integrating chemical delivery channels with electrical and optical fibers has been a challenge. To address this issue, Xie's group developed multifunctional neural probes by conformal attachment of nanoelectronic coating devices to the surface of a glass pipet [194], while other groups integrated microfluidic channels in the neural recording device using MEMS or microcontact printing fabrication methods [207,208]. These technologies involve multiple fabrication steps, and are difficult to scale up to multiple channels. To overcome these challenges, fiber thermal drawing method has been adopted to produce scalable multifunctional probes [38]. These multifunctional fiber probes with simultaneous electrical recording, optical stimulation, and drug delivery capabilities also enable optogenetic experiments in wild-type animals using a single-step surgery [66]. (Fig. 10l). This technology, combined with wireless communication and micropump technologies, can open new opportunities in closed-loop systems for disease intervention and treatment.

Scaffolding fibers for nerve repair and regeneration

The versatility in the design and fabrication of multimaterial fibers makes them advantageous for tissue engineering applications. Hollow-core fibers with various channel geometries were fabricated and used for nerve axonal guidance (Fig. 10m) [209]. Furthermore, to enhance the media exchange and oxygen flow across the scaffold, porous fiber scaffolds were produced using phase separation during the fiber drawing [73] (Fig. 10o). More recently, a porous fiber scaffold was developed using a salt-leaching method [210] (Fig. 10n). This fiber was then fused into

a 3D printing system to create multichannel microporous scaffolds at centimeter scales. In addition to geometrical guidance, many other methods have been shown to be effective in promoting neurite growth, such as growth factor delivery [211], electrical stimulation [212], optogenetic stimulation, and the application of electric fields [213], all of which can potentially be adopted into a multimaterial fiber scaffold. Besides, simultaneous electrical recording can be used for monitoring the progress of nerve growth [214,215]. In the future, multimaterial scaffolding fibers with added electrical and optical modalities can provide an effective and scalable platform for nerve repair and regeneration.

Despite the short history of multimaterial fiber-based neural interfaces, prominent progress has been made in this field, showing great promise for both basic and clinical neuroscience applications. Looking forward, there are still many unanswered questions to be addressed. Firstly, the backend connection needs to be improved for scalable applications. Secondly, the electrode impedance needs to be further reduced to minimize the device footprint. Thirdly, multisite interfacing remains a big challenge in fiber-based probes. Methods need to be developed to create multiple interface sites along the fiber, which can significantly enhance the applications of these devices. Moreover, other functionalities that mimic the brain complexity can be integrated into the fibers, including chemical sensing, mechanical adaptive, acoustic, and biodegradable properties. Last but not least, applications in the peripheral nervous system and other organs are also largely unexplored fields in which multimaterial multifunctional fibers can play an important role.

Multimaterial fibers for micro- and nanofabrication

While in many cases thermally-drawn fibers are treated as functional devices with transitional symmetry where both fiber materials and geometries are identical to those in the fiber preform, they also act as an unprecedented micro- and nanofabrication platform where fiber materials or geometries are altered for in-situ chemical reaction, in-situ phase transformation as well as materials structuring including micro-/nanowire and micro-/nanospheres fabrication, thanks to their unparalleled small cross-section, large aspect ratio, tunable material diversity, and confined inner core of the multimaterial fibers. All these fibers can also be used as the building blocks for 3-D printing of complex structure as we detail in section 7.5.

Laser restructuring high-temperature semiconductor-core optical fibers

High-temperature semiconductors such as Si, Ge, SiGe and GaSb are of technological importance because of their unique nonlinear optical properties, optoelectronic effects and transparent windows [216–218]. High-temperature semiconductor-core optical fibers are emerging as unique platforms for all-in-fiber electronic, optic and optoelectronic devices. Thermal drawing of high-temperature semiconductors into fibers involves melting and solidification in a random manner, leading to polycrystalline crystal formation. The small cross-section and large aspect ratio of the fiber provides a unique platform to tailor the microstructure of the semiconductors using post-drawing processes. Recent progress has focused on controlling the crystallinity, crystallographic orientation, compositional segregation and induced stress of the core materials via laser-based resolidification [48,218–221]. In this section, we will introduce how breaking fiber axial symmetry via post-fabrication laser processing create novel fibers containing technologically important materials in-situ formed during laser processing, as well as generate peculiar phenomena for fundamental studying interesting topics in materials science and physics.

Using a CO_2 laser to form a large temperature gradient that suppresses crystal nucleation at the solidification front, Coucheron et al. reported the fabrication of large monocrystalline SiGe-core optical fibers [48]. Constitutional undercooling is suppressed by controlling the translation rate of the laser, which allows the solid/liquid interface to advance with a planar morphology and without microsegregation occurring in the alloy. The same method has been exploited to fabricate Si- and Ge-core optical fibers with long single crystals. Very recently, Prof. Ursula Gibson at the Norwegian University of Science and Technology incorporates GaSb acting as an excellent optical material into Si-core optical fibers [75]. The as-drawn fiber exhibits a classic eutectic microstructure with thin interspersed GaSb in the Si matrix. The Si grows with the <1 1 1> direction parallel to the fiber axis. The GaSb surprisingly grows epitaxially in the host Si, showing the same preferential spatial orientation. Using a CO_2 laser to re-structure the as-drawn fiber, they realize the segregation of the biphasic microstructure into single constituent domains. The ability to isolate III–V crystalline semiconducting materials within the Si core might open opportunities for the integration of light sources within IR light-transmitting silicon optical fibers.

Another intriguing application of using lasers to structure semiconductor-core optical fibers is to induce a large stress in crystalline materials. The highly confined geometry of the fiber system makes it possible to incorporate high stress into the core. Healy et al. reported that tensile stress up to 5 GPa is induced in a silicon crystal lattice when using a continuous-wave visible laser to remelt the silicon core [74]. Such a high stress modifies the electronic band structure with a bandgap reduction from 1.11 eV down to 0.59 eV, enabling optical detection up to 2100 nm. This in-fiber confined solidification technique is also employed for the in-fiber spherical particles that were formed via the Plateau-Rayleigh instability. Gemennik et al. reported that a uniform GPa-scale hydrostatic stress is incorporated in solidified silicon spheres, independent of their diameters, when heating the silicon core via a CO_2 laser to induce capillary breakup [71]. The resulting strain field alters the refractive index and caused the materials to become birefringent. This is also a promising method to set stress other functional materials, such as Ge and SiGe.

In-fiber new materials synthesis

Fibers can act as reaction vehicles. Chemicals can be introduced into the fiber to react with one another under certain defined conditions. The products of the chemical reaction either stay in the fiber and serve as a working component in the newly formed structure or are purged outside of the fiber in the form of a vapor or molten mixture.

It is still considerably challenging to cover more kinds of materials in the fiber device system. To expand the material selection and enhance the fiber device performance, researchers have examined the possibility of introducing new materials into the fiber via other means, for instance, via chemical vapor deposition in the as-drawn fiber or via a chemical reaction inside the fiber during the drawing process [44,45,72,166,167,222–224].

The concept of using the fiber as a high-pressure microfluidic reactor was firstly reported in 2006, when Sazio et al. deposited silicon and germanium in the core of a silica-clad fiber using a high-pressure chemical vapor deposition (HPCVD) method [167]. Sparks et al. also demonstrated the use of the HPCVD method to deposit the compound zinc selenide (ZnSe) inside a silica-clad fiber [222]. It involves the chemical reaction between dimethylzinc (DMZn), dimethylselenide (DMSe) and hydrogen. Using the same method, more complicated structures, such as a silicon p-i-n junction inside the silica-clad fiber, have also been produced and shown photovoltaic and photodetection properties [166]. On the other hand, silicon core fibers can be directly fabricated using the molten-core method [225]. The addition of silicon carbide (SiC) to the silicon core [223] provides an *in situ* reactive oxygen getter during the drawing process, and the resulting fiber had less oxygen content in the core area. Hou et al. observed a more dramatic change in the composition of the fiber core, in which the pure silicon-core, silica-clad fiber was made from an aluminum-core preform [45]. The chemical reaction inside the fiber has not only been studied in silica-clad fibers but also in polymer-clad fibers. Orf et al. found that the compound ZnSe could be synthesized during drawing a polymer-clad fiber. The $Se_{97}S_3$ thin film contacts the $Sn_{85}Zn_{15}$ metallic electrodes, reacts and yields ZnSe at the interface. An improvement on the yield of ZnSe adds more Zn to the reaction system by alternatively evaporating 50-nm-thick Zn and 1-μm-thick $Se_{97}S_3$ films. This method significantly increases the volume of ZnSe produced and enables an unambiguous material characterization [72].

In-fiber nanowire fabrication

While the preform serves as a microcrucible for a chemical reaction and new material formation, it also allows one to modify the geometry rather than the material composition during thermal drawing. In particular, Deng and his colleagues first discovered that the initially intact cylindrical thin film shell breaks up along the circumferential direction into an ordered array of filaments, while uniformity is maintained in the axial direction [67]. This occurs when the thickness of the thin film reaches a critical value. Dense nanofilaments with extremely long lengths can be harvested by dissolving the polymer cladding, which provides an innovative approach for the mass production of nanowires. A fluid front instability mechanism is proposed to account for the observed phenomena. The fluid instability is then systematically explored from the perspective of the classical Plateau-Rayleigh instability mechanism [226]. Considering that the instability happened at the microscopic length scale, van der Waals forces are supposed to play a role. Very recently, Deng and his colleagues further proposed a physical model by taking into account both van der Waals forces and the effect of stretching to understand such anisotropic instability [227]. Based on linear stability analysis, this model elegantly predicts an enhanced transverse instability and a suppressed longitudinal instability that led to the filament formation. Moreover, their predication remarkably agrees well with experimental observations. This work not only provides deep insight into a long-lasting theoretical issue in the field of fiber electronics, but also sheds light on the design of complex micro- and nanostructured devices in fibers and textiles. Another straightforward way to produce nanowires in fibers is via the iterative thermal drawing approach [68,228]. Fibers obtained from previous draws are embedded in new preforms and are repeatedly drawn, resulting in a continuous size reduction of active materials inside the fibers. Semiconducting nanowires with a feature size down to a few nanometers are produced while maintaining axial continuity.

In-fiber micro- and nanoparticle fabrications

Micro-and nanoparticles offer great opportunities for biomedical applications, such as drug delivery [229], medical diagnostics [230], tissue engineering [231], and other applications, such as cosmetics, optical coatings [232] and environmental remediation [233]. Typical applications require various particle sizes and morphologies. To date, conventional top-down methodologies, such as microfluidic-based approaches [234] and lithography [235], can produce monodisperse particles with better control over the morphologies than their chemical-dependent bottom-up counterparts, but they are still limited in applications by the inherent kinetics, such as the dependency on the prefabricated devices, the deficiency of production capability and morphology control. The lack of control over the modality in conventional methodologies can be concluded as the main difficulty in obtaining suitable 'micro- and nanoscale hands' to operate materials at the micro- or nanoscale. The great developments in multimaterial fibers have provided us with a unique tool to allocate diverse material systems. By arranging structures and materials in the preform in a complex LEGO-like manner [236], further reducing the dimension to the desired magnitude by thermal drawing (or by iterative fiber drawing [68]), Tao et al. created relatively suitable 'hands' at the micro- and nanoscale without sophisticated prefabricated devices.

The deficiency of production capability is another problem. Silica optical fibers play a major role in miniaturizing our world. Considering that the length of submarine cables constructed on Earth is several times that of the equator, fiber fabrication technology, mostly referred to as thermal fiber drawing (Fig. 11a), can be considered as one of the most scalable and mature fabrication approaches. Naturally, leveraging a high-throughput and precious multimaterial fiber fabrication approach could be a promising pathway to enhance the capability of production (from conventional mg/h to kg/h scales), exceptionally widen the range of the particle size (from millimeter to nanometer) and improve the control over the modality. We combine the inherently scalable and facile thermal fiber drawing approach with two kinds of intriguing but quite simple fabrication methodologies to yield multimaterial particles with a wide range of scales and complex geometries.

Proposed in 2012 by Kaufman et al. the first in-fiber micro- and nanoparticle fabrication method [69] is known as the Plateau-Rayleigh Instability (PRI)-induced breakup [237]

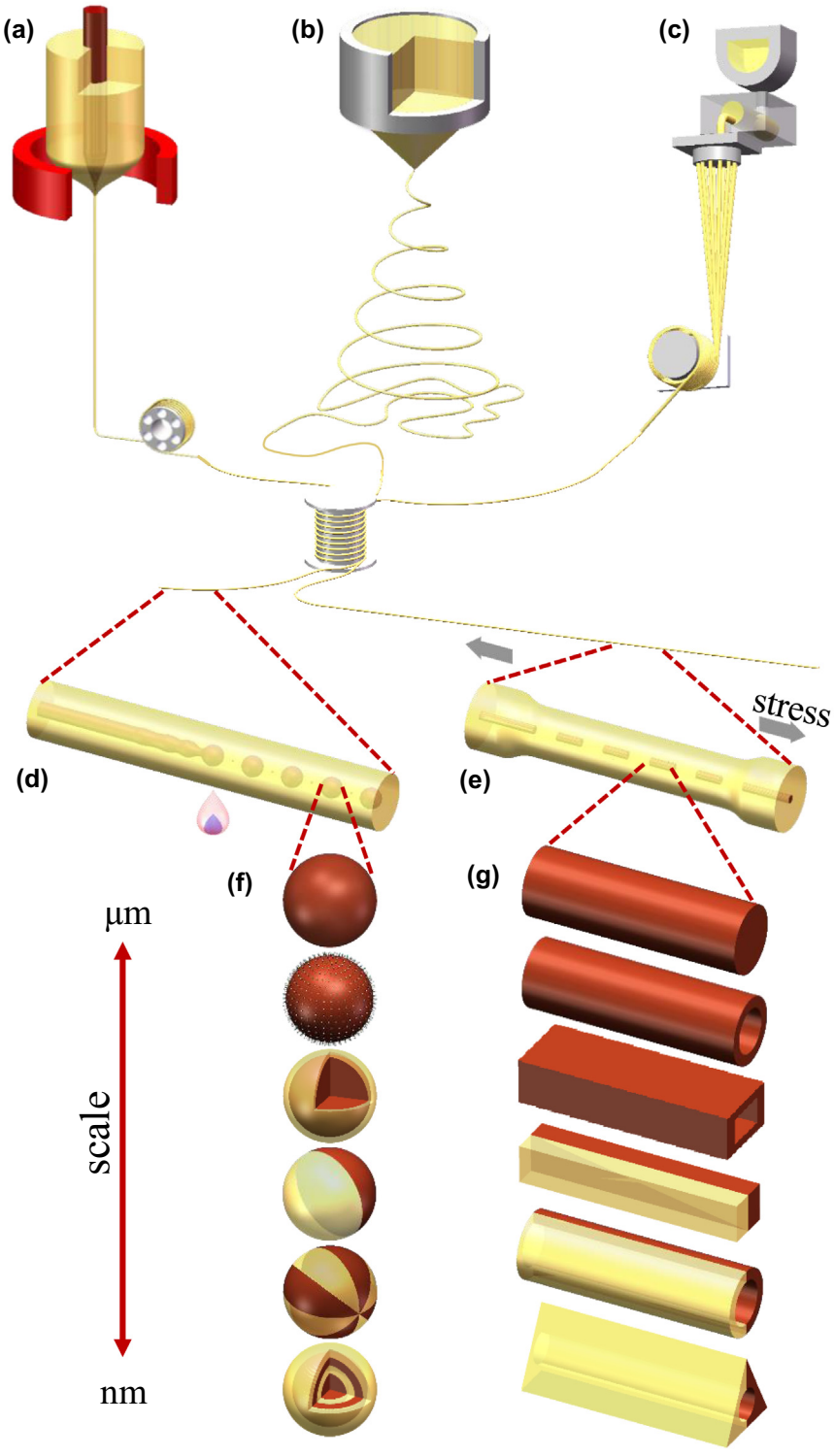

FIGURE 11

(a–c) Schematic illustrations of three types of novel fiber fabrication techniques including thermal fiber drawing, electrospinning and melt spinning. (d, e) Schematic illustrations of the in-fiber micro- and nanoparticle fabrication methodologies, including the PRI-induced breakup and the Polymer Cold Drawing. The gray arrows indicate the direction of applied external stress and the directions of shoulder propagation. (f) and (g) are the schematic illustrations of functionalized spherical particles produced by the PRI-induced breakup in (d) and non-spherical particles produced by polymer cold drawing in (e).

(Fig. 11d), which occurs in daily scenarios as the formation of droplets. When heated above the glass transition temperature, the complex core turns into the soften phase. Dominated by the surface tension at the interface of the core phase and the cladding matrix, the continuous core phase gradually forms into a necklace of oriented spherical particles. The diverse morphologies of multimaterial particles fabricated from multimaterial fibers are shown in Fig. 11f. A group of potential applications,

such as tunable optical scattering [236], biosensing, drug delivery [238], heavy metal recovery, cell recognition and separation [239], have been shown by four kinds of engineering methods: radial, azimuthal or combined structure engineering, impregnation of functional materials, surface functionalization, and functional material encapsulation. Considering that the modality relies on the rheology of the materials, this methodology is independent of the chemistry, which means that it can involve a variety of material systems, as mentioned above. Another recent developed In-fiber micro- and nanoparticle fabrication method is cold drawing of multimaterial fibers [51], shown in Fig. 11e. The cold drawing is a time-honored methodology in polymer industrial applications. By forming a cladding over the brittle core in ductile polymers, under the applied tensile stress, the intact core fragments into a train of rods within the fiber. The length-to-diameter ratio can be tuned by changing the cross-section geometries. Release could be performed to yield the resultant columnar particles with the same cross-sectional geometry as that of the initial fibers (Fig. 11f).

This '1 dimension to 0 dimension' (fibers to particles) methodologies can also be combined with other scalable and controllable fiber fabrication approaches, such as melt spinning [240] and electrospinning [241] (Fig. 11b and c), and such particle fabrication methodologies can be even more scalable. With a deeper exploitation of material science and rheology, more intriguing functions, such as magnetron robots, can be endowed to single micro- and nanoparticles. Furthermore, creating an array of a variety of structured particles is also maps out an exciting pathway towards the next generation of functional devices.

Fibers as multimaterial device ink

Printing metals, insulators, and semiconductors concurrently into a device is challenging due to difficulties in enabling these material classes to adhere well each to form intimate device interfaces. In addition, each of these material classes have different physical properties, necessitating the combination of different deposition hardware thus resulting in the printer to be bulky and complex. Loke et al. [76] reported a new approach that harnesses these multimaterial fibers (Fig. 12a–f) as an ink, and a regular desktop 3D-printer, to print three-dimensional devices. Key to this approach is to utilize the thermoplastic cladding of these multimaterial fibers as the adhesive promotor for individual deposited fibers to adhere well to each other. The authors also introduce a new print approach termed filament surface heating that aims to heat only the surface of the fiber, while the core, which contains the device structure, can remain unaffected when printing. Through this approach, three-dimensional structure of any form factors can be constructed to exhibit device functionality. For instance, a three-dimensional closed sphere printed from a photodetecting fiber is capable of spatially detecting light impingement at any position on the sphere surface (Fig. 12c, d), enabling applications for solar cell tracking and robotic eyes. The authors then demonstrate the printing of both light-emitting and light-detecting fibers into a single structure. A model airplane wing (Fig. 12e) is printed with light-emitters at the top and bottom layer, while light-detectors are printed within the middle layers. One application of such a bi-functional wing is its ability to interrogate defect at any position within the wing. This is enabled by comparing the photocurrent before and after the defect is made to the printed photodetecting fiber (Fig. 12f). Through this functional structure, catastrophic structural failure from these defects can thus be prevented. This holds much promise for applications where high mechanical stresses are commonly encountered, for example drones, prosthetics and mobile vehicles. It is noted that this print approach is not only applicable towards printing optoelectronic fibers. For instance, using this approach, thermally drawn porous fibers are used to print customized scaffolds of shapes that match the gaps in the spinal cords or bifurcated nerves [242]. These scaffolds contain a hierarchy of structures, ranging from large microchannels to small pores, to enable highly accelerated nerve regeneration across the scaffold.

Integration of multimaterial fibers into electronic textiles

One important technological application of fiber electronics is using them as the building blocks for electronic textiles. While ubiquitous, textiles have remained their functionality unchanged for thousands of years. Recent tremendous efforts have been transforming this conventional form into electronic devices or smart systems. Thermally drawn electronic fibers possess several intriguing assets for the realization of electronic textiles. The fabrication method is simple and complex device architecture is simply designed at the macroscopic preform level. The approach is highly scalable yielding large-scale functional fibers that can be directly integrated into textiles using conventional textile processes such as weaving, knitting, embroidery and stitching. The polymer cladding that encapsulates the inner electronics can be water-proof, enabling fibers to be washable under many cycles. Some good examples include a textile integrated with thermal-sensing fibers capable of mapping the skin temperature, and textiles containing thermoelectric fibers holding great promise to modulate human body temperature, as we show in Fig. 6. In Fig. 9, we also show recent progress on smart textiles integrating diodes fibers for optical communications. Systematic study demonstrates that the fibers show identical performance as before weaving or the washing cycle tests. The unique mechanical properties of cladding materials would add more values to the textile products. One impressive example is that the stretchable fiber cladded by soft SEBS exhibit extraordinary mechanical robustness, as we mention in Section 4.2. Such fibers maintain high performance after subjecting them to 10^5 stretching cycles. A variety of harsh deformations such as twisting, shearing, or fast and large force impingement have insignificant effect on the properties of these fibers. Under 15 standard washing cycles from the textile industry fibers remain the same functionalities. All these examples show that thermally-drawn fibers might enable a new generation of electronic textiles.

Besides direct integration of electronic fibers into textiles for the fabrication of electronic textiles, other typical technology include embedding electronic devices onto textile substrates and direct functionalization of textile surfaces using conventional approaches such as coating, deposition, spinning or printing. The former approach is straightforward because all electronic devices in industry can be leveraged. However, encap-

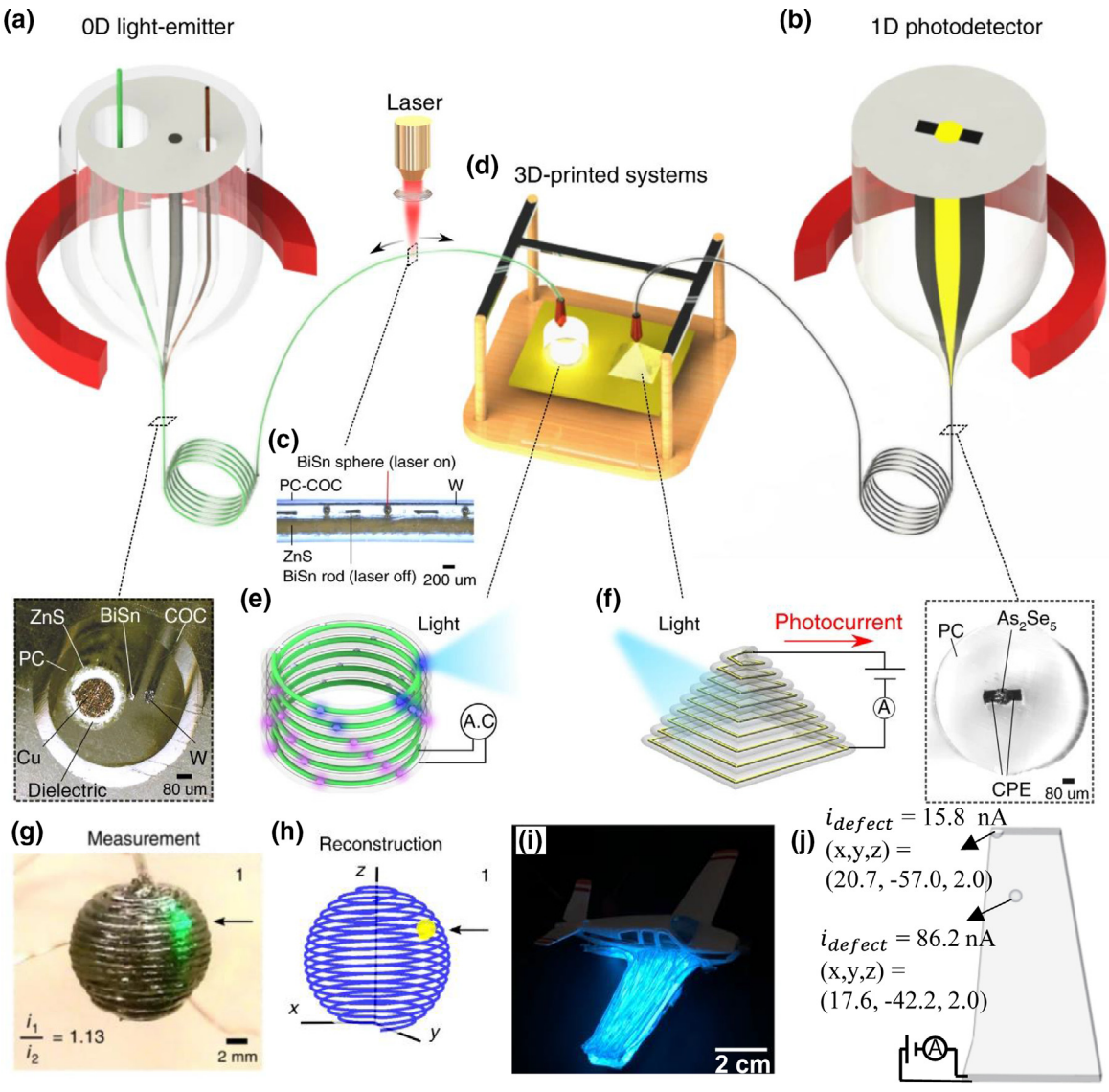

FIGURE 12

(a, b) Thermal-drawing of (a) light-emitting and (b) light-detecting fibers, encapsulating metals, semiconductors, and insulators within their cross-sections. (c) Laser-processing is used to fabricate capillary spheres that operate as pixels within the filaments. The image shows the planar optical micrograph of the fiber after laser-processing. (d) These multimaterial fibers are fed into a regular printer, enabling the printing of three-dimensional (e) light-emitting and (f) light-detecting devices. (g) An omnidirectional photodetecting sphere, capable of localizing point of light impingement anywhere on its surface. (h) The reconstruction of light on the sphere. (i) A bi-functional light-emitting and light-detecting model airplane wing, capable of localizing defect point anywhere within the bulk of the wing. (j) Localizing of two defect points within the airplane wing by measuring the photocurrent before and after the defects are made Copyright 2019, Nature Publishing Group.

sulation of these devices, electrically or optically connecting the integrated functionalities, as well as the capability of sustaining many wash cycles remains challenging. The latter approach is versatile because various technological functional materials including high-performance carbon-based nanomaterials and metallic nanomaterials can be harnessed. In this regard, great success has been achieved in making 1D textile-based electrodes. However, to form an electronic system in textiles, other more complex components such as capacitors, resistors, transistors, antennas and circuitry should also be developed. We will not give a detailed review on these two technology, but instead refer the reader to a variety of important review articles [125,243–250].

Conclusion and outlook

The thermally drawn advanced functional fibers that integrate electronic and optoelectronic functionalities open up a wide range of potential applications in a variety of technological fields, including sensing, communications, energy, robotics, smart textiles, bioengineering and neuroscience. The underlying science provides great opportunities for many research areas of fundamental interest, including materials processing, control over structure at the atomic and micro-levels and property optimization, the integration of different materials with disparate physical and chemical properties, rheology and interface science, and the coupling of multiple functionalities. The integration of

electronic fibers with/within traditional textiles might revolutionize textile-based technology and industry. By leveraging artificial intelligence (AI), electronic fibers and textiles might evolve into more smart systems. We conclude this work with some perspectives on the remaining challenges and future directions as follows:

(1) *Fabrication:* The thermal drawing process itself is highly simple and scalable since the principle is the same as that of optical fiber manufacturing in industry. However, the fabrication processes of preforms are incompatible with existing electronic technologies. The development of more advanced and integrated technologies, such as 3-D printing [251], are required.

(2) *Materials:* Despite the great success achieved over the past 20 years, the available functional materials that can be integrated into the thermally drawn fiber platform are limited. Different thermal, mechanical, rheological and surface properties of different materials impose restrictions on the process. A recent fundamental understanding of the interplay between surface tension and viscosity sheds new light on processing thermally drawn materials [252]. On the other hand, new technologies [52] developed very recently are rapidly integrating various functional materials that seem to be incompatible with the thermal drawing process into the fiber platform.

(3) *Performance:* The material microstructure determines its properties and thus the device performance. Research on the interplay between materials structure and material properties is just beginning and is emerging as an exciting field for fundamental and applied research. To achieve complex functionalities, tremendous efforts have been made in the design of sophisticated fiber architectures. A strategy to circumvent the fabrication of a complex fiber architecture is to desirably control the atomic and microstructure of electronic materials. One example is a fluorescence imaging application enabled by an optoelectronic fiber that integrates high-performance monocrystalline semiconducting nanowires synthesized via engineering the interfacial energy of crystal planes [50]. Another example is laser restructuring, leading to the Si/GaSb heterojunction in a semiconductor-core optical fiber [75]. Efforts along this direction are expected to result in more intriguing opportunities both in fundamental and applied research.

(4) *Functionalities:* Thriving research momenta in the field of fiber and textiles from the academia, industries, government and funding agencies led to the creation of Advanced Functional Fabrics of America (AFFOA), which is the 8th public–private partnership of the National Network for Manufacturing Innovation in the United States. As a Revolutionary Fibers and Textiles Manufacturing Innovation Hub, AFFOA aims to design, develop and manufacture next generation of smart fibers and textiles. The functions of fibers will escalate in a predictable way, forming the context for a "Moore's law" analogue in fibers and textiles. It is predicted that in the next years, fibers integrating a number of devices will be able to see, hear, sense, communicate, store and convert energy, regulate temperature, monitor health and change color. Indeed, increasing the density of optical, electronic and optoelectronic devices in multimaterial fibers makes them more functional. In addition to enriching the database of materials compatible with thermal drawing, new technological platforms enabling the direct incorporation of prefabricated materials and devices into fibers are increasingly required. A recent breakthrough has realized a package of hundreds of light-emitting and photodetecting diode chips into a single strand of fiber for both telecommunication and health monitoring.

(5) *Integration of fiber electronics into textiles:* As we show in Fig. 1, multimaterial functional fiber electronics can be seamlessly integrated with fabrics or textiles whose functionalities have maintained unchanged for thousands of years to generate next-generation of smart textiles. Wearing such fabrics, human will be able to obtain physiological information such as blood pressure level, PH and chemical constituents of sweat, body temperature and heart beating rate anytime at anywhere. Mechanical information such as bending, twisting, stretching and rotation can also be obtained from deformation fiber sensors. Triboelectric, piezoelectric and photovoltaic fibers can harvest energy from the vibration, movement, friction and the sun. The energy can immediately power the sensors or can be stored in the fiber batteries or supercapacitors, allowing the whole system to be self-powered. Under emergency, fabrics with LED fibers or optical fibers can emit urgency signals or communicate with others.

Compared with electronic sensing systems, optical sensing schemes provide some unique strengths in fast response and remote signal transmission. In particular, textiles based on fiber optical technology for health monitoring have been developed very fast over the past decades, making detecting human vital signs such as heart rate, respiration, blood pressure and sugar, and ballistocardiograph (BCG) readings possible and reliable [253–257]. Combining optical sensing with electronic sensing into an integrated system will overcome many challenges in respective areas and thus largely accelerate the intelligence of textiles.

(6) *Artificial Intelligence enabling smart electronic textiles:* The ability to integrate and connect fiber-based sensors, LEDs, energy harvesters, batteries/supercapacitors and other electronic components within wearable textiles and clothing is endowing textiles and clothing with the capability of collecting and transmitting data. Compared with rigid wearable devices, the data acquisition process of clothing and textiles using intelligent fabric technology is more transparent and more accurate, and data quality is more reliable and more realistic. Intelligent fabrics will have great potential if they are combined with AI technologies with powerful data processing and analysis abilities. Below, we will introduce AI-intelligent fabric from four aspects: data acquisition, data storage and uploading, data analysis and response to users (as shown by Fig. 13), which might provide perspective for future research on AI-intelligent fabric.

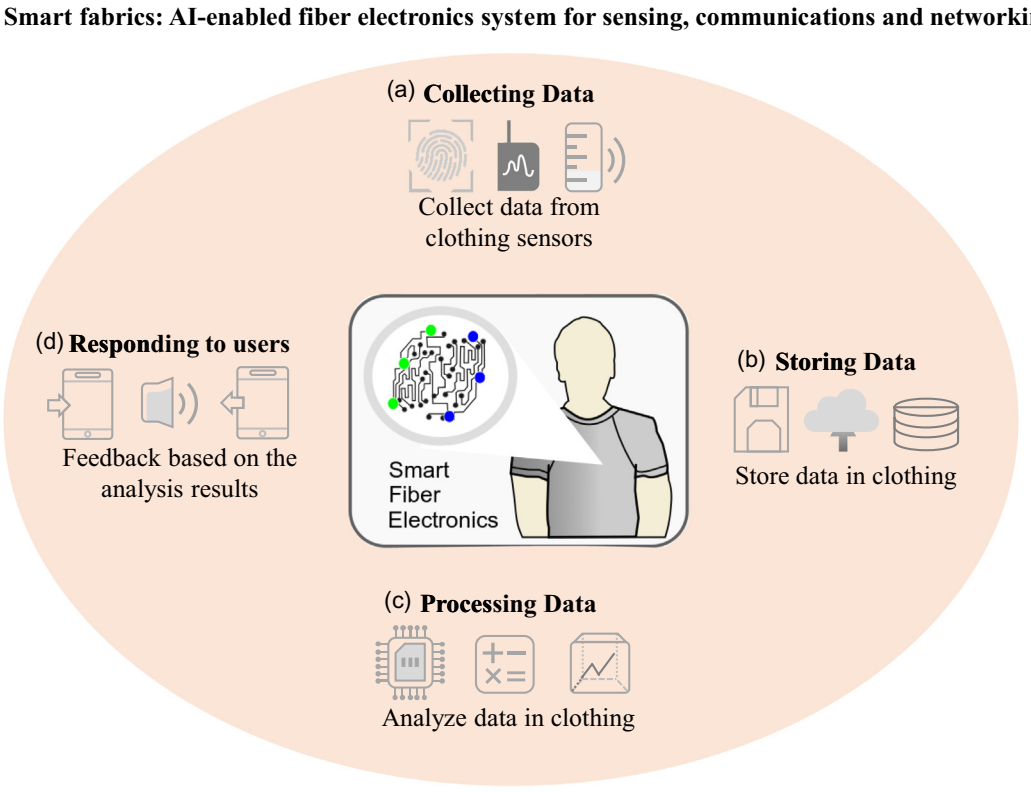

FIGURE 13

Conceptual idea of smart electronic textiles enabled by artificial Intelligence.

a) *Data acquisition:* Using flexible sensors spreading over smart fabrics, one can collect more precise physical and physiological signals from human body. These sensors acquire user data closer to the user. The user data include fingerprint data, body data, heartbeat, breathing and even motor muscle data. Moreover, unlike most existing wearable devices that only possess simplified functions, the use of intelligent fabrics can enable more comprehensive functions through designing a variety of sensors at any locations of the fabric circuit in clothing and textile accessories. Thus, multi-modal, multi-angle and omni-directional understanding of users will be realized, providing reliable data support for AI technology.

b) *Data storage and uploading:* In the process of data acquisition, how to store these constantly generated data in a safe and effective way is important. One strategy is to build micro-network data centers on fabrics based on micro-memory. Micro-memory installed in the suitable location of intelligent fabric can store data temporarily, reducing the network burden and transmission delay caused by data transmission back and forth in the cloud. When the amount of data reaches a certain threshold, data can be uploaded to the cloud for backup. After the data backup is completed, the micro-memory is cleaned up, only leaving the key data necessary for real-time tasks.

c) *Data analysis:* Intelligent fabric systems combined with sensors and circuit components can be regarded as a micro computing center. Firstly, the data collected by sensors are processed and cleaned. Communications built between user's mobile devices and sensors then transmit data to the corresponding apps and provide feedback directly to the user. In addition, AI algorithm can also be used to mine deep information. Tasks can either be deployed locally or in the cloud, depending on the requirements of storage and computing resources. For example, when the training and enhancement of the model takes a long time, and the demand for resources is high, tasks will be deployed in the cloud. These tasks mainly use AI technologies such as deep learning and reinforcement learning to analyze and mine data in depth. When low latency and high availability are more important in responding to users' tasks, data will be deployed locally. One example is that cloud-trained models downloaded directly to the local processor process real-time data for regression classification and provide feedback to users.

d) *Response to users:* Only by providing feedback of the analysis results of data to users can the value of data processing be realized, so responding to users is also a very important part. The response mode of users is closely related to the functions and scenes of intelligent fabrics. Assuming that intelligent fabrics are used in sports scenes, AI-intelligent fabrics can make individualized training plans for athletes according to their physical conditions in daily training. In the competition, the coach can track the state of the players in real time and adjust the tactics or personnel in time. When intelligent fabrics are applied in educational scenarios, students can not only make appropriate learning plans, but also provide feedback of their learning status to teachers and/or parents to help themselves better manage their learning and life styles.

Successful outcomes from these efforts will have the potential to fundamentally change our concept of fibers and textiles.

Fibers and textiles are evolving from the form of being a single material with a single function into highly integrated electronics exhibiting complex structure and functionalities. Combining thermally drawn fiber technology with computation and Artificial Intelligence, we believe that fibers and associated textiles integrating optical, sensing, photovoltaic, thermoelectric, piezoelectric, and triboelectric functions and batteries and supercapacitors will help deliver the next generation of smart flexible and wearable electronics.

Acknowledgements

The authors would like to acknowledge Meifang Zhu, Xinliang Zhang and Jun Zhou for their encouragement, support, and vision. Guangming Tao acknowledges the National Natural Science Foundation of China (Grant No. 61875064), WNLO Man-Machine Lab Fund, WNLO Innovation Fund and HUST Innovation Fund (Grant No. 2172018KFYXKJC021). Run Hu acknowledges the National Natural Science Foundation of China (Grant No. 51606074). Lei Wei acknowledges the Singapore Ministry of Education Academic Research Fund Tier 2 (MOE2015-T2-2-010), and Singapore Ministry of Education Academic Research Fund Tier 1 (MOE 2019-T1-001-103 and MOE2019-T1-001-111). Shifeng Zhou acknowledges the National Key R&D Program of China (2018YFB1107200), National Natural Science Foundation of China (Grant No. 51622206, 51972113), and the Key Program of Guangzhou Scientific Research Special Project (201904020013). Xiaoting Jia acknowledges the National Science Foundation under Grant No. 1847436. Xiaoming Tao acknowledges Research Grants Council (152110/16E and 152009/17E) and Innovation and Technology Commission (ITS/306/17) of Hong Kong SAR Government. Fabien Sorin acknowledges the Swiss CCMX Materials Challenge funding scheme, the Swiss National Science Foundation (Grant No. 200021_146871), and the European Research Council (ERC Starting Grant 679211 "FLOWTONICS").

Data availability

There are no linked research data sets for this submission. The following reason is given: No data were used for the research described in the article.

References

[1] A. Abouraddy et al., Nat. Mater. 6 (5) (2007) 336.
[2] H. Sun et al., Nat. Rev. Mater. 2 (6) (2017) 17023.
[3] W. Zeng et al., Adv. Mater. 26 (31) (2014) 5310.
[4] D. Yu et al., Chem. Soc. Rev. 44 (3) (2015) 647.
[5] A. Cusano et al., Lab-on-Fiber Technology, Springer, 2015.
[6] X.-M. Tao, Study of Fiber-Based Wearable Energy Systems, Acc. Chem. Res. 52 (2) (2019) 307.
[7] J. Ren et al., Flex. Print. Electron. 3 (1) (2018) 013001.
[8] X. Xu et al., The Rise of Fiber Electronics, Angew. Chem. 131 (2019) 2.
[9] A. Leber et al., Adv. Funct. Mater. 29 (5) (2019) 1802629.
[10] J. Shi et al., Smart Textile-Integrated Microelectronic Systems for Wearable Applications, Adv. Mater. 1901958 (2019).
[11] Smart fibres, fabrics and clothing: fundamentals and applications. Elsevier: 2001
[12] Handbook of Smart Textiles. Springer: Singapore, 2015
[13] Z. Liu et al., Adv. Mater. 30 (5) (2018) 1704229.
[14] B. Zhang et al., Adv. Funct. Mater. 28 (29) (2018) 1801683.
[15] Y. Guo et al., Nano Energy 48 (2018) 152.
[16] X. Chen et al., Nano Energy 38 (2017) 43.
[17] W. Weng et al., Angew. Chem. Int. Ed. 55 (21) (2016) 6140.
[18] J.R. Sparks et al., Ann. Rev. Mater. Res. 43 (2013) 527.
[19] M. Tebyetekerwa et al., Energy Environ. Sci. (2019).
[20] X. He et al., Adv. Funct. Mater. 27 (4) (2017) 1604378.
[21] N. Matsuhisa et al., Nat. Commun. 6 (2015) 7461.
[22] G. Kostovski et al., Adv. Mater. 26 (23) (2014) 3798.
[23] K. Dong et al., ACS Nano 11 (9) (2017) 9490.
[24] J. Ryu et al., Nano Energy 55 (2019) 348.
[25] J. Zhong et al., ACS Nano 8 (6) (2014) 6273.
[26] S. Pan et al., J. Phys. Chem. C 118 (30) (2014) 16419.
[27] Z. Zhao et al., Adv. Mater. 28 (46) (2016) 10267.
[28] L. Liu et al., Angew. Chem. Int. Ed. 56 (35) (2017) 10471.
[29] W. Ma et al., J. Power Sources 306 (2016) 481.
[30] P. Li et al., Adv. Mater. 30 (18) (2018) 1800124.
[31] J. Ren et al., Angew. Chem. Int. Ed. 53 (30) (2014) 7864.
[32] J. Ren et al., Adv. Mater. 25 (8) (2013) 1155.
[33] X. Li et al., ACS Nano 8 (10) (2014) 10674.
[34] X. Fu et al., J. Mater. Chem. A 6 (1) (2018) 45.
[35] Q. Pei et al., Science 269 (5227) (1995) 1086.
[36] H. Zheng et al., Nat. Commun. 10 (1) (2019) 2790.
[37] W. Yan et al., Adv. Mater. 31 (1) (2019) 1802348.
[38] A. Canales et al., Nat. Biotechnol. 33 (3) (2015) 277.
[39] J. Lee et al., Adv. Mater. 27 (15) (2015) 2433.
[40] A. Gumennik et al., Adv. Mater. 24 (45) (2012) 6005.
[41] G. Tao et al., Int. J. Appl. Glass Sci. 3 (4) (2012) 349.
[42] B. Temelkuran et al., Nature 420 (6916) (2002) 650.
[43] S.D. Hart et al., Science 296 (5567) (2002) 510.
[44] N.D. Orf et al., Proc. Natl. Acad. Sci. USA 108 (12) (2011) 4743.
[45] C. Hou et al., Nat. Commun. 6 (2015) 6248.
[46] S. Danto et al., Adv. Mater. 22 (37) (2010) 4162.
[47] F. Sorin et al., Multi-material optoelectronic fiber devices, Proc. ISOP, 10194, 2017, p. 1019407.
[48] D.A. Coucheron et al., Nat. Commun. 7 (2016) 13265.
[49] F. Sorin et al., Multi-material and multi-functional optical fibers, in: Proc. OSA, 2018, p. Tu2J. 6.
[50] W. Yan et al., Adv. Mater. 29 (27) (2017) 1700681.
[51] S. Shabahang et al., Nature 534 (7608) (2016) 529.
[52] M. Rein et al., Nature 560 (7717) (2018) 214.
[53] M. Bayindir et al., Nature 431 (7010) (2004) 826.
[54] M. Bayindir et al., Nat. Mater. 4 (11) (2005) 820.
[55] A.F. Abouraddy et al., Nat. Mater. 5 (7) (2006) 532.
[56] F. Sorin et al., Nano Lett. 9 (7) (2009) 2630.
[57] A.M. Stolyarov et al., Nat. Photonics 6 (4) (2012) 229.
[58] M. Bayindir et al., Adv. Mater. 18 (7) (2006) 845.
[59] S. Egusa et al., Nat. Mater. 9 (8) (2010) 643.
[60] S. Danto et al., Adv. Funct. Mater. 21 (6) (2011) 1095.
[61] Y. Qu et al., Adv. Mater. 30 (27) (2018) 1707251.
[62] T. Khudiyev et al., Nat. Commun. 8 (1) (2017) 1435.
[63] R. Yuan et al., Proc. Natl. Acad. Sci. USA 115 (46) (2018) E10830.
[64] T. Zhang et al., Nano Energy 41 (2017) 35.
[65] M. Kanik et al., Science 365 (6449) (2019) 145.
[66] S. Park et al., Nat. Neurosci. 20 (4) (2017) 612.
[67] D. Deng et al., Nano Lett. 8 (12) (2008) 4265.
[68] M. Yaman et al., Nat. Mater. 10 (7) (2011) 494.
[69] J.J. Kaufman et al., Nature 487 (7408) (2012) 463.
[70] L. Wei et al., Adv. Mater. 29 (1) (2017) 1603033.
[71] A. Gumennik et al., Proc. Natl. Acad. Sci. USA 114 (28) (2017) 7240.
[72] C. Hou et al., Nano Lett. 13 (3) (2013) 975.
[73] B. Grena et al., Nat. Commun. 8 (1) (2017) 364.
[74] N. Healy et al., Nat. Mater. 13 (12) (2014) 1122.
[75] S. Song et al., Nat. Commun. 10 (1) (2019) 1790.
[76] G. Loke et al., Nat. Commun. 10 (1) (2019) 4010.
[77] Y. Fink et al., Science 282 (5394) (1998) 1679.
[78] P.G. Isaza et al., Int. Urogynecol. J. 29 (2) (2018) 211.
[79] L. Rindorf et al., Opt. Express 14 (18) (2006) 8224.
[80] C. Cheng et al., ACS Appl. Mater. Interfaces 2 (7) (2010) 1824.
[81] W. Zhou et al., Sci. Rep. 8 (1) (2018) 14866.
[82] Y.M. Park et al., J. Laparoendosc. Adv. A 19 (3) (2009) 361.
[83] M.S. de Cumis et al., Opt. Express 22 (23) (2014) 28222.
[84] G. Benoit et al., Adv. Mater. 15 (24) (2003) 2053.
[85] G. Benoit et al., Opt. Lett. 30 (13) (2005) 1620.

[86] R.R. Gattass et al., Opt. Express 24 (22) (2016) 25697.
[87] S.K. Alavipanah et al., Criteria of selecting satellite data for studying land resources, Desert 15 (2010) 83.
[88] S. Aalam et al., Experimental investigations on a CRDI system assisted diesel engine fuelled with aluminium oxide nanoparticles blended biodiesel, Alexandria Eng. J. 54 (3) (2015) 351.
[89] A. Kołodziejczak-Radzimska et al., Structural Characterisation of ZnO Particles Obtained by the Emulsion Precipitation Method, J. Nanomater. 2012 (2012) 656353.
[90] M. Jung et al., Validation of ATR FT-IR to identify polymers of plastic marine debris, including those ingested by marine organisms, Marine Pollution Bull. 127 (2018) 704.
[91] F. Nürnberg et al., Bulk damage and absorption in fused silica due to high power laser applications, Proc. SPIE 9632 (2015) 96321R.
[92] S.R. Bowman et al., Opt. Mater. Express 8 (4) (2018) 1091.
[93] A. Rogalski, HgCdTe infrared detector material: history, status and outlook, Reports on Progress in Physics, 2005. p. 2267.
[94] B. Matveev et al., Sensors Actuators B: Chem. (1998) 233.
[95] A. Rogalski, History of infrared detectors, Opto-Electron. Rev. 20 (3) (2012) 279.
[96] R. Garg, Handbook of Laser Wavelengths, CRC Press (2000) 62.
[97] Y. Yao et al., Nat. Photon. (2012) 432.
[98] A.M. Stolyarov et al., Appl. Phys. Lett. 101 (1) (2012) 011108.
[99] N. Zhang et al., ACS Photonics 3 (12) (2016) 2275.
[100] W.C. Wang et al., Prog. Mater. Sci. 101 (2019) 90.
[101] J. Chen et al., Adv. Opt. Mater. 7 (6) (2019) 1801413.
[102] G. Tang et al., Opt. Mater. Express 9 (2) (2019) 362.
[103] G. Tang et al., Opt. Lett. 44 (13) (2019) 3290.
[104] W. Wang et al., Opt. Express 27 (8) (2019) 10438.
[105] S. Zhou, J. Qiu, MRS Bull. 42 (1) (2017) 34.
[106] Y. Yu et al., NPG Asia Mater. 8 (2016) e318.
[107] Y. Huang et al., Opt. Express 26 (15) (2018) 19171.
[108] J. Deng et al., Carbon 149 (2019) 63.
[109] L. Sun et al., Ionogel-based, highly stretchable, transparent, durable triboelectric nanogenerators for energy harvesting and motion sensing over a wide temperature range, Nano Energy 63 (2019) 103847.
[110] A. Takemoto et al., Nanotechnology 30 (37) (2019) 37LT03.
[111] W. Li et al., ACS Appl. Energy Mater. 2 (4) (2019) 2803.
[112] H. Xian et al., Nanotechnology 30 (8) (2018) 085705.
[113] M. Pruvost et al., NPJ Flex. Electron. 3 (1) (2019) 7.
[114] M.R. Crump et al., Nanotechnology 30 (36) (2019) 364002.
[115] S.S. Mechael et al., Flex. Print. Electron. 3 (4) (2018) 043001.
[116] W. Wu, Sci. Technol. Adv. Mater. 20 (1) (2019) 187.
[117] S. Lv et al., Adv. Opt. Mater. 6 (21) (2018) 1800881.
[118] W. Yan et al., Multi-material optical fibers with integrated optoelectronic devices, Proc. OSA, 2016. p. AF3A.3.
[119] T. Nguyen-Dang et al., J. Phys. D 50 (14) (2017) 144001.
[120] N. Bartolomei et al., Super-elastic multi-material optical fibers for healthcare applications, Optical Fibers and Sensors for Medical Diagnostics and Treatment Applications XIX 10872 (2019). p. 108720M.
[121] Y. Qu et al., Super elastic optical fibers sensors, Proc. OSA, 2018. p. ThE66.
[122] M.D. Dickey, Adv. Mater. 29 (27) (2017) 1606425.
[123] C.B. Cooper et al., Adv. Funct. Mater. 27 (20) (2017) 1605630.
[124] A. Frutiger et al., Adv. Mater. 27 (15) (2015) 2440.
[125] J. Lee et al., Adv. Mater. (2019) 1902532.
[126] J. Lee et al., Adv. Mater. 27 (15) (2015) 2433.
[127] S. Lee et al., Adv. Funct. Mater. 25 (21) (2015) 3114.
[128] N. Chocat et al., Adv. Mater. 24 (39) (2012) 5327.
[129] S. Wang et al., Adv. Electron. Mater. 3 (3) (2017) 1600449.
[130] Y. Zhang et al., J. Mater. Chem. A 5 (4) (2017) 1415.
[131] T. Chen et al., Angew. Chem. Int. Ed. 50 (8) (2011) 1815.
[132] Y. Fu et al., Energy Environ. Sci. 4 (9) (2011) 3379.
[133] Z. Lv et al., Nanoscale 4 (4) (2012) 1248.
[134] K. Dong et al., Adv. Mater. (2019) 1902549.
[135] Y. Hu, Z. Zheng, Nano Energy 56 (2019) 16.
[136] C. Dong et al., Adv. Mater. Technol. (2019) 1900417.
[137] B. Chen et al., Adv. Mater. Technol. 3 (11) (2018) 1800175.
[138] G. Lestoquoy et al., Appl. Phys. Lett. 102 (15) (2013) 152908.
[139] S. Gorgutsa et al., Smart Mater. Struct. 21 (1) (2011) 015010.
[140] T. Zhang et al., Adv. Electron. Mater. 3 (4) (2017) 1600554.
[141] T. Zhang et al., ACS Appl. Mater. Interfaces 11 (2) (2018) 2441.
[142] M. Carrara et al., Radiat. Meas. 56 (2013) 312.
[143] Q. Guo et al., IEEE Photonic Technol. 29 (2) (2017) 251.
[144] X. Xu et al., ACS Appl. Mater. Interfaces 10 (45) (2018) 39238.
[145] S. Lv et al., ACS Appl. Mater. Interfaces 9 (24) (2017) 20664.
[146] S.J. Gerbode et al., Science 337 (6098) (2012) 1087.
[147] T. Mirfakhrai et al., Mater. Today 10 (4) (2007) 30.
[148] T.D. Gupta et al., Self-assembly of nanostructured glass metasurfaces via templated fluid instabilities, Nat. Nanotechnol. 14 (4) (2019) 320.
[149] T.D. Gupta et al., Template assisted dewetting of optical glasses for large area, flexible and stretchable all dielectric metasurfaces, Conference on Lasers and Electro-Optics, Optical Society, Optical Society of America, San Jose, California, 2018. p. STh1I.5.
[150] F. Sorin et al., Nano-structured optical metasurfaces and multi-material fibers for IR applications, Proc. IEEE, 2019. p. 1.
[151] F. Sorin et al., Adv. Mater. 19 (22) (2007) 3872.
[152] F. Sorin et al., Opt. Express 18 (23) (2010) 24264.
[153] W. Yan et al., Opt. Mater. Express 7 (4) (2017) 1388.
[154] W. Yan et al., J. Phys. Chem. C 122 (43) (2018) 25134.
[155] W. Yan et al., Integration of high-performance optoelectronic nanowire-based devices at optical fiber tips, Proc. OSA, 2018. p. SF2K. 4.
[156] J.-L. Wang et al., Adv. Mater. 30 (48) (2018) 1803430.
[157] T. Güner et al., Nanotechnology 29 (13) (2018) 135202.
[158] D. Ren et al., Nanotechnology 30 (29) (2019) 294001.
[159] J. Ballato et al., Opt. Express 18 (5) (2010) 4972.
[160] J. Ballato et al., Opt. Fiber Technol. 16 (6) (2010) 399.
[161] A. Peacock et al., Adv. Phys. X 1 (1) (2016) 114.
[162] T. Lühder et al., J. Lightwave. Technol. 37 (13) (2019) 3244.
[163] Z. Zhao et al., Opt. Fiber Technol. 41 (2018) 193.
[164] M. Rein et al., Nat. Commun. 7 (2016) 12807.
[165] R. He et al., Nat. Photonics 6 (3) (2012) 174.
[166] R. He et al., Adv. Mater. 25 (10) (2013) 1460.
[167] P.J. Sazio et al., Science 311 (5767) (2006) 1583.
[168] E.S. Boyden et al., Nat. Neurosci. 8 (9) (2005) 1263.
[169] A.M. Aravanis et al., J. Neural Eng. 4 (3) (2007) S143.
[170] F. Zhang et al., Nat. Rev. Neurosci. 8 (2007) 577.
[171] K. Deisseroth, Nat. Methods 8 (2010) 26.
[172] F. Zhang et al., Nat. Protoc. 5 (2010) 439.
[173] J. Tønnesen et al., Proc. Natl. Acad. Sci. USA 106 (29) (2009) 12162.
[174] M. Zhao et al., Epilepsy Res. 116 (2015) 15.
[175] Y. Lu et al., Nat. Commun. 7 (2016) 10962.
[176] K.T. Vann, Z.-G. Xiong, Int. J. Physiol. Pathophysiol. Pharmacol. 8 (1) (2016) 1.
[177] C. Armstrong et al., Nat. Protoc. 8 (2013) 1475.
[178] E. Krook-Magnuson et al., Nat. Commun. 4 (2013) 1376.
[179] J.T. Paz et al., Nat. Neurosci. 16 (2012) 64.
[180] K. Schulz et al., Nat. Methods 9 (2012) 597.
[181] Lisa A. Gunaydin et al., Cell 157 (7) (2014) 1535.
[182] C.K. Kim et al., Nat. Methods 13 (2016) 325.
[183] B.A. Flusberg et al., Nat. Methods 2 (12) (2005) 941.
[184] B.A. Flusberg et al., Nat. Methods 5 (2008) 935.
[185] M. Murayama et al., J. Neurophysiol. 98 (3) (2007) 1791.
[186] K. Tamura et al., J. Neurosci. Methods 211 (1) (2012) 49.
[187] P. Anikeeva et al., Nat. Neurosci. 15 (1) (2012) 163.
[188] I. Ozden et al., J. Neurosci. Methods 219 (1) (2013) 142.
[189] J. Wang et al., J. Neural Eng. 9 (1) (2011) 016001.
[190] J. Zhang et al., J. Neural Eng. 6 (5) (2009) 055007.
[191] S. Royer et al., Eur. J. Neurosci. 31 (12) (2010) 2279.
[192] S. Dufour et al., PLOS ONE 8 (2) (2013) e57703.
[193] Y. LeChasseur et al., Nat. Methods 8 (2011) 319.
[194] Z. Zhao et al., Nano Lett. 17 (8) (2017) 4588.
[195] F. Wu et al., Neuron 88 (6) (2015) 1136.
[196] M. Schwaerzle et al., J. Micromech. Microeng. 27 (6) (2017) 065004.
[197] H. Lee et al., J. Neural Eng. 2 (4) (2005) 81.
[198] A. Sridharan et al., J. Neural Eng. 10 (6) (2013) 066001.
[199] A. Gilletti, J. Muthuswamy, J. Neural Eng. 3 (3) (2006) 189.
[200] R. Fu et al., Adv. Opt. Mater. 6 (3) (2018) 1700941.
[201] R. Nazempour et al., Materials (Basel) 11 (8) (2018) 1283.
[202] J.-W. Jeong et al., Cell 162 (3) (2015) 662.
[203] Y. Guo et al., ACS Nano 11 (7) (2017) 6574.
[204] C. Lu et al., Adv. Funct. Mater. 24 (42) (2014) 6594.
[205] C. Lu et al., Sci. Adv. 3 (3) (2017) e1600955.
[206] C. Dagdeviren et al., Sci. Transl. Med. 10 (425) (2018) eaan2742.
[207] H.J. Lee et al., Lab Chip 15 (6) (2015) 1590.
[208] A. Altuna et al., Lab Chip 13 (2013) 1422.
[209] R.A. Koppes et al., Biomaterials 81 (2016) 27.
[210] D. Shahriari et al., Adv. Mater. 31 (30) (2019) 1902021.

[211] A.A. Al-Majed et al., Cell. Mol. Neurobiol. 24 (3) (2004) 379.
[212] D.M. Thompson et al., Annu. Rev. Biomed. Eng. 16 (1) (2014) 397.
[213] K.M. Musick et al., Sci. Rep. 5 (2015) 14363.
[214] F.J. Rodríguez et al., J. Neurosci. Methods 98 (2) (2000) 105.
[215] A.C. Peacock et al., Laser Photonics Rev. 8 (1) (2014) 53.
[216] N. Healy et al., Semicond. Sci. Technol. 33 (2) (2018) 023001.
[217] Z. Zhao et al., Opt. Mater. Express 9 (3) (2019) 1333.
[218] N. Healy et al., Adv. Opt. Mater. 4 (7) (2016) 1004.
[219] X. Ji et al., ACS Photonics 4 (1) (2016) 85.
[220] J. Ballato et al., Opt. Express 17 (10) (2009) 8029.
[221] J.R. Sparks et al., Adv. Mater. 23 (14) (2011) 1647.
[222] S. Morris et al., Opt. Mater. Express 1 (6) (2011) 1141.
[223] J. Ballato et al., Opt. Mater. Express 2 (2) (2012) 153.
[224] J. Ballato et al., Opt. Express 16 (23) (2008) 18675.
[225] D. Deng et al., Opt. Express 19 (17) (2011) 16273.
[226] B. Xu et al., Phys. Rev. Fluids 4 (7) (2019) 073902.
[227] J.J. Kaufman et al., Nano Lett. 11 (11) (2011) 4768.
[228] R.M. Ottenbrite, S.W. Kim, Polymeric Drugs and Drug Delivery Systems, CRC Press, 2019.
[229] A. Sandhu, H. Handa (Eds.), Magnetic Nanoparticles for Medical Diagnostics, IOP Publishing, 2018.
[230] A. Hasan et al., Int. J. Nanomedicine 13 (2018) 5637.
[231] H. Hottel et al., AIAA J. 9 (10) (1971) 1895.
[232] K. Mondal, A. Sharma, RSC Adv. 6 (87) (2016) 83589.
[233] J. Wang et al., Micromachines 8 (1) (2017) 22.
[234] B. Bhushan, Springer Handbook of Nanotechnology, Springer, 2017.
[235] G. Tao et al., Proc. Natl. Acad. Sci. USA 113 (25) (2016) 6839.
[236] X. Liang et al., J. Fluid Mech. 683 (2011) 235.
[237] J.J. Kaufman et al., Proc. Natl. Acad. Sci. USA 110 (39) (2013) 15549.
[238] M. Du et al., ACS Nano 12 (11) (2018) 11130.
[239] E. Stojanovska et al., RSC Adv. 6 (87) (2016) 83783.
[240] J. Xue et al., Electrospinning and Electrospun Nanofibers: Methods, Materials, and Applications, Chem. Rev. 119 (8) (2019) 5298.
[241] D. Shahriari et al., Adv. Mater. (2019) 1902021.
[242] W. Weng et al., Adv. Mater. (2019) 1902301.
[243] X. Xu et al., Angew. Chem. Int. Ed. 58 (39) (2019) 13643.
[244] L. Wang et al., Adv. Mater. (2019) 1901971.
[245] B. Wang, A. Facchetti, Adv. Mater. 31 (28) (2019) 1901408.
[246] S.C. Dhanabalan et al., Nanoscale 11 (7) (2019) 3046.
[247] T. Hughes-Riley et al., Fibers 6 (2018) 2.
[248] A.K. Yetisen et al., ACS Nano 10 (3) (2016) 3042.
[249] C. Faccini de Lima et al., Nanoscale Res. Lett. 14 (1) (2019) 209.
[250] T. Nguyen-Dang et al., Adv. Funct. Mater. 27 (10) (2017) 1605935.
[251] Z. Liu et al., Photonics 6 (2019) 2.
[252] Q. Chai et al., Opt. Eng. 58 (7) (2019) 1.
[253] K. Bhowmik, G.-D. Peng, Polymer optical fibers, in: G.-.D. Peng (Ed.), Handbook of Optical Fibers, Singapore, Springer Singapore, 2019, p. 1.
[254] G. Woyessa et al., Opt. Mater. Express 7 (1) (2017) 286.
[255] D.Q. Ying et al., Smart Mater. Struct. 22 (1) (2012) 015004.
[256] W. Zheng et al., Text. Res. J. 84 (17) (2014) 1791.
[257] L. Dziuda et al., J. Biomed. Opt. 18 (5) (2013) 1.